made to preserve the biventricular physiology in neonates or early infants with symptomatic Ebstein's anomaly since the introduction of the Starnes' concept. A functioning RV should be able to generate a pressure difference between the RV and RA in the systolic phase and, thus, cause some antegrade main pulmonary arterial (PA) flow. We believe that the presence of the trans-TV systolic pressure difference of >30 mmHg, an antegrade main pulmonary blood flow and a good non-atrialized RV morphology are indicators of a positive potential for restoring RV function. Thus, biventricular repair (BVR) at the time of the first surgical intervention in patients with these preoperative findings should still be considered. Here, we aimed to describe the outcomes of symptomatic neonatal Ebstein's anomaly achieved in this institution and to determine whether our treatment strategy could be beneficial for avoiding the future establishment of Fontan circulation in these patients.

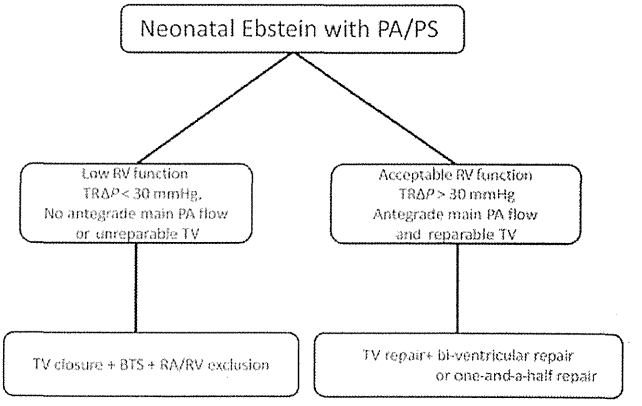

Figure 1: The management of symptomatic patients with neonatal Ebstein's anomaly at Okayama University Hospital. If the patient has a pressure difference of >30 mmHg in the systolic phase between the RV and the RA and a repairable TV, a biventricular or one-and-a-half repair is performed. In other cases, the patient undergoes TV closure with BT shunt application.

PATIENTS AND METHODS

Study subjects

We retrospectively reviewed the medical and surgical records of neonates with symptomatic Ebstein's anomaly who required surgical intervention in the neonatal or early infant period in Okayama University Hospital between June 1999 and November 2010.

Data collection and measurements

This study was approved by the Institutional Research Ethics Board at Okayama University Hospital, and patient consent was waived. Data collected from the medical records included patient demographics, cardiac diagnosis, clinical condition, previous procedures, operative data as well as postoperative and follow-up clinical status, including catheter and echocardiographic data. The pressure difference between the RV and RA was determined by the Doppler flow velocity of the tricuspid regurgitation (TR) as follows: $PG = 4 \times v2$ (PG: pressure gradient between the RV and RA; v: velocity of the TR flow as measured by echocardiography).

Selection of patient management

Our basic strategy is shown in Fig. 1. If a patient could be managed with oral medication, no surgical treatment was performed in the neonatal or early infant period. These patients were considered candidates for BVR. If patients could not be managed with oral medication, an early surgical intervention was indicated. The patients were considered as candidates for BVR or one-and-a-half repair when a trans-TV systolic pressure difference of >30 mmHg was observed on echocardiography and TV repair was possible. In these cases, TV repair and RV outflow reconstruction with/without a modified BT shunt were performed as an initial operation. If the patient was a suitable candidate, a one-stage BVR was performed. When the pressure difference was <30 mmHg or TV repair was not feasible, the patients were considered as suitable candidates for the Fontan operation. In these cases, a TV closure with fenestration, RV/RA exclusion and application of a modified BT shunt were performed as an initial operation.

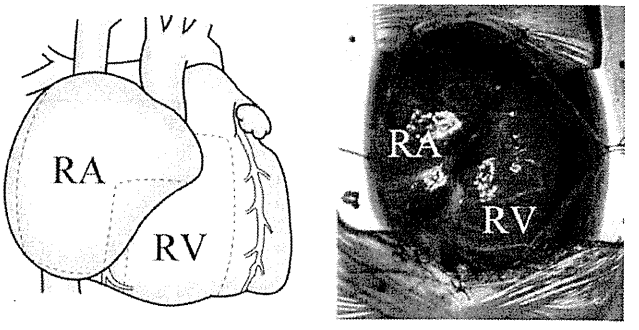

Figure 2: Total RV and RA exclusion of neonatal Ebstein's anomaly. The RV and RA are excluded along the dotted lines suggested here. RA: right atrium. RV: right ventricle.

Surgical procedures

If the patients needed a modified BT shunt with/without a pulmonary valvotomy and had good arterial oxygen saturation, the operation was performed without cardiopulmonary bypass (CPB). The BT shunt was created either from the innominate artery to the right PA or from the left subclavian artery to the left PA via a thoracotomy, using a 4-mm extended polytetrafluoroethylene (ePTFE) graft. A PA valvotomy was performed with clamping of the main PA.

If patients required CPB, the operation was performed using a conventional continuous flow CPB with moderate hypothermia (24–34°C) via a standard median sternotomy. CPB was established with bicaval drainages or an RA single venous drainage with an ascending aortic return. If needed, the RA was opened, and intracardiac repair was performed. The TV repair technique was selected according to the surgeon's preference.

The exclusion of the RV free wall was performed as previously described [4]. The TV was closed with a fenestrated ePTFE patch (the fenestration was created with a 3- or 4-mm puncher) or autologous TV tissue (Figs 2 and 3). When the TV was closed with autologous TV tissue, a small hole was left as a fenestration (a 3- or 4-mm Hegar dilator could be passed through it).

In cases of one-stage BVR, all associated cardiovascular anomalies were corrected, including closure of a ventricular septal defect (VSD) with a Dacron sauvage or ePTFE patch using 6-0 pledgeted

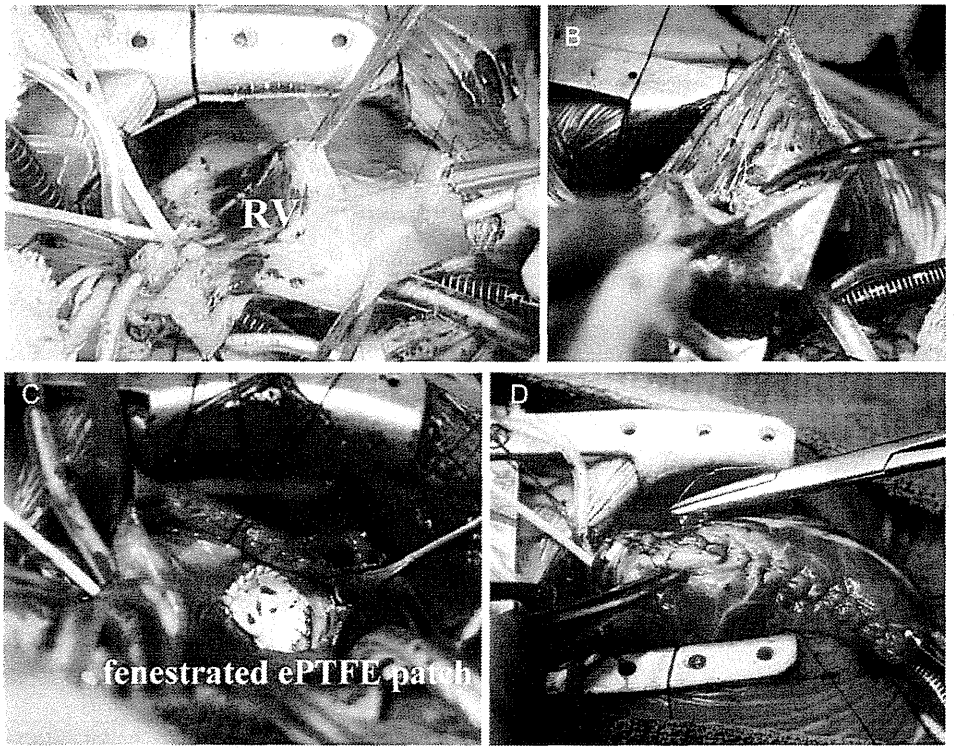

Figure 3: Images of an RV exclusion procedure. A 14-day old patient with an Ebstein's anomaly; the patient's body weight was 2.0 kg (Patient 12). (**A**) A paper-thin RV free wall. (**B**) The RV free wall was excised to reduce the size of the RV cavity. (**C**) The TV was closed with a fenestrated ePTFE patch. The blood in the coronary sinus was drained into the RA. (**D**) The RV free wall was closed directly, and a modified BT shunt was placed. BT shunt: Blalock-Taussig shunt. ePTFE graft: polytetrafluoroethylene graft. RV: right ventricle.

polypropylene sutures; closure of an atrial septal defect (ASD) or a patent foramen ovale (PFO), with 6-0 polypropylene running sutures; and repair of coarctation of the aorta (CoA), in an extended end-to-end fashion using 8-0 polypropylene running sutures.

Data analysis

Data are expressed as the mean ± SD or the median and range as appropriate. The Kaplan–Meier method was used to determine the estimated patient survival.

RESULTS

Patient characteristics

Twelve symptomatic neonates with Ebstein's anomaly were treated at our institute between June 1999 and November 2010. The mean gestational age was 38 ± 3 (range, 32–41) weeks. The mean birth body weight was 2.85 ± 0.46 (range, 2.29–3.56) kg. The mean cardio-thoracic ratio (CTR) on chest radiography was 80 ± 14% (range, 57–98%). Seven patients were born by normal delivery and 5 were delivered by Caesarean section. Table 1 summarizes the patient characteristics. According to Carpentier's classification of the Ebstein's anomaly, we noted that 2 patients were type A, 5 were type B and 5 were type C. TR was mild in 2 (17%) patients, moderate in 1 (8%) and severe in 9 (75%). True pulmonary atresia was observed in 7 patients, functional atresia in 1 and severe pulmonary stenosis in 1. These 9 patients received prostaglandin E1 infusions for maintaining pulmonary blood flow after birth. For 3 patients, the estimated trans-TV systolic pressure difference between the RV and RA by echocardiography was <20 mmHg. One patient had severe myocardial calcification that was detected after the first operation by a computerized tomography scan. The associated extracardiac anomalies included Down syndrome in 2 patients, anal atresia in 1, idiopathic chylous ascites in 1, hypertrophy of the adrenal glands in 1 and calcification of the kidney in 1.

Surgical data

All patients underwent open heart surgery in the neonatal stage (7 patients) or in early infancy (5 patients). Six (50%) patients required mechanical respiratory ventilator support preoperatively. At the initial operation, the mean age, body weight and body surface area were 29 ± 25 (range, 5–92) days, 2.81 ± 0.54 (range, 2.04–4.05) kg and 0.18 ± 0.02 (range, 0.15–0.22) m^2, respectively.

Five patients, aged 5–92 days, underwent a one-stage BVR (Patients 1–5 in Table 1). The TV repair methods for these 5 patients were Hardy's procedure in 2, Carpentier's procedure in 1, Cone's reconstruction in 1 and plasties of the septal and posterior leaflet in 1 patient with a dysplastic anterior leaflet (Fig. 4). The associated procedures included patch closure of a VSD in 3 patients, direct closure of an ASD or PFO in 4, semiclosure of an ASD in 1, repair of CoA in 1, and RV outflow reconstruction with pulmonary valvotomy and RV outflow muscle resection in 2.

The remaining 7 patients received a modified BT shunt with an ePTFE graft as palliative treatment via a median sternotomy

Table 1: Summary of the cardiac conditions and outcomes

No.	Carpentier's classification	Associated cardiovascular anomaly	TR	RVOTO	RV systolic function	1st Op	RV ex	Final status	Outcome
1	A	CoA, VSD, ASD	Trivial	No	Normal contraction with VSD	BVR	No	BVR	Alive
2	B	VSD, ASD, PDA, PAPVD	Severe	No	Normal contraction with VSD	BVR	No	BVR	Alive
3	B	VSD, ASD,	Severe	No	PG = 48 mmHg	BVR	No	BVR	Alive
4	B	Severe PS, PDA, ASD, PLSVC	Severe	PS	PG = 43 mmHg	BVR	No	BVR	Alive
5	C	PA/IVS, PDA, PFO	Severe	PA	PG = 53 mmHg	BVR	No	BVR	Alive
6	B	PA/IVS, PDA, PFO	Severe	PA	Mild plastering	BTS	No	BVR	Alive
7	B	PA/IVS, PDA, PFO	Severe	PA	No data	BTS	No	BTS	Dead
8	C	HypoRV, PFO, PS (small PV with normal leaflets)	Trivial	PS	Obvious antegrade mPA flow	BTS	No	1 + 1/2	Alive
9	C	PA/IVS, PDA, PFO	Severe	PA	PG = 4 mmHg	BTS	Yes	TCPC	Dead
10	A	PA/IVS, PDA, PFO	Moderate	PA	PG = 185 mmHg	BTS	No	BVR	Alive
11	C	PA/IVS, PDA, PFO	Severe	PA	PG = 9 mmHg	BTS	Yes	BDG	Alive
12	C	PA/IVS, PDA, ASD	Severe	PA	PG = 15 mmHg	BTS	Yes	BTS	Alive

ASD: atrial septal defect; BDG: bidirectional Glenn operation; BTS: Blalock-Taussig shunt; BVR: biventricular repair; CoA: coarctation of the aorta; hypoRV: hypoplastic right ventricle; PA: pulmonary atresia; PA/IVS: pulmonary atresia with an intact ventricular septum; PAPVD: partial anomalous pulmonary venous drainage; PDA: patent ductus arteriosus; PG: pressure gradient; PFO: patent foramen ovale; PLSVC: persistent left superior veno cava; PS: pulmonary stenosis; PV: pulmonary valve; RV ex: total right ventricular exclusion; RVOTO: right ventricular outflow tract obstruction; sys.: systolic; TCPC: total cavopulmonary connection; TR: tricuspid regurgitation; VSD: ventricular septal defect; 1st Op: first-stage operation.

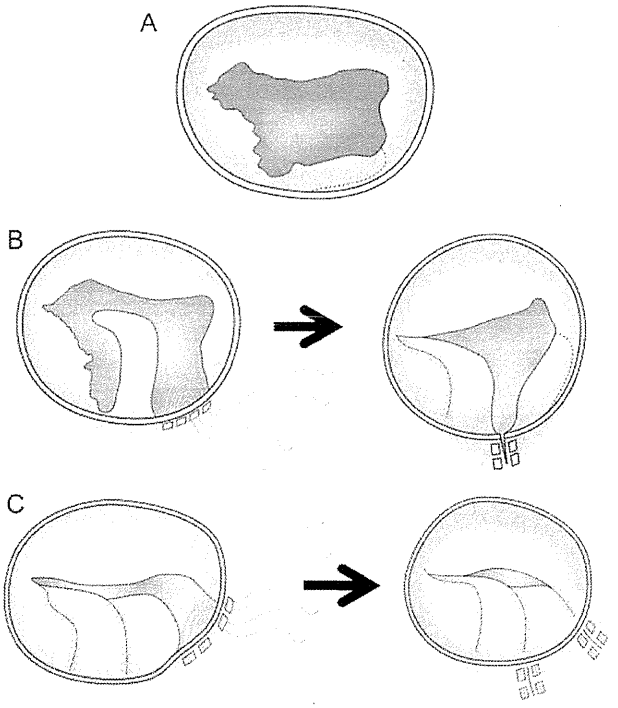

Figure 4: TV plasty with dysplastic septal and posterior leaflets and a non-sail-like anterior leaflet in Patient 4. (A) The septal and posterior leaflets were severely dysplastic. The anterior leaflet was also mildly dysplastic and lacked sufficient area for monocuspization. The fused or dysplastic chordae of the septal leaflet were divided to create a free area for the septal leaflet. The created free septal leaflet was subsequently partially cut off from the annulus (dotted line). (B) The created free leaflet was rotated counterclockwise and sutured to the leaflet. Thereafter, an annuloplasty using pledgeted polypropylene sutures was performed. The posterior leaflet was then partially cut off from the annulus (dotted line). (C) The free leaflet was rotated counterclockwise and sutured, and an annuloplasty using pledgeted polypropylene sutures was consequently performed.

(5 patients) or a thoracotomy (2 patients) at the age of 7–50 days. The diameter of the ePTFE graft used was 3.0 mm in 2 patients, 3.5 mm in 2 and 4.0 mm in 3. CPB was established in 4 of the 7 patients. The associated procedures consisted of RV/RA exclusion in 3 patients, plication of the RA in 1, creation of an ASD in 1, closure of the TV using autologous TV tissue with fenestration in 2 and TV with a fenestrated ePTFE patch in 1.

Postoperative outcomes

Figure 5 illustrates the patient flow chart about the selected surgical technique and the outcomes. Four of the 12 patients were believed to have low RV function and were considered as Fontan candidates. However, the other 8 patients were estimated to have acceptable RV function and were considered as suitable candidates for BVR or one-and-a-half repair.

One case of early death occurred because of sepsis (Patient 7 in Table 1). This patient's age at the first intervention was 43 days; he was born at a gestational age of 41 weeks and had a body weight of 2.62 kg at birth. Moreover, he had true pulmonary atresia with an intact ventricular septum (PA-IVS), a PFO and severe TR. He was found to have a CTR of 98%, as indicated by chest radiography. Prostaglandin E1 was administered immediately after birth to open the arterial duct. He had a persistently increased white blood cell count and C-reactive protein (CRP) level before the operation. However, because he had heart failure due to high PA flow and because the increase in the white blood cell count and CRP level was very mild, the patient underwent application of a 3-mm modified BT shunt, ligation of the arterial duct and plication of the RA via a median sternotomy. TV repair was not performed because of the risk of postoperative deterioration due to infection resulting from CPB. However, this patient experienced septic shock in the early postoperative period and died on the seventh postoperative day.

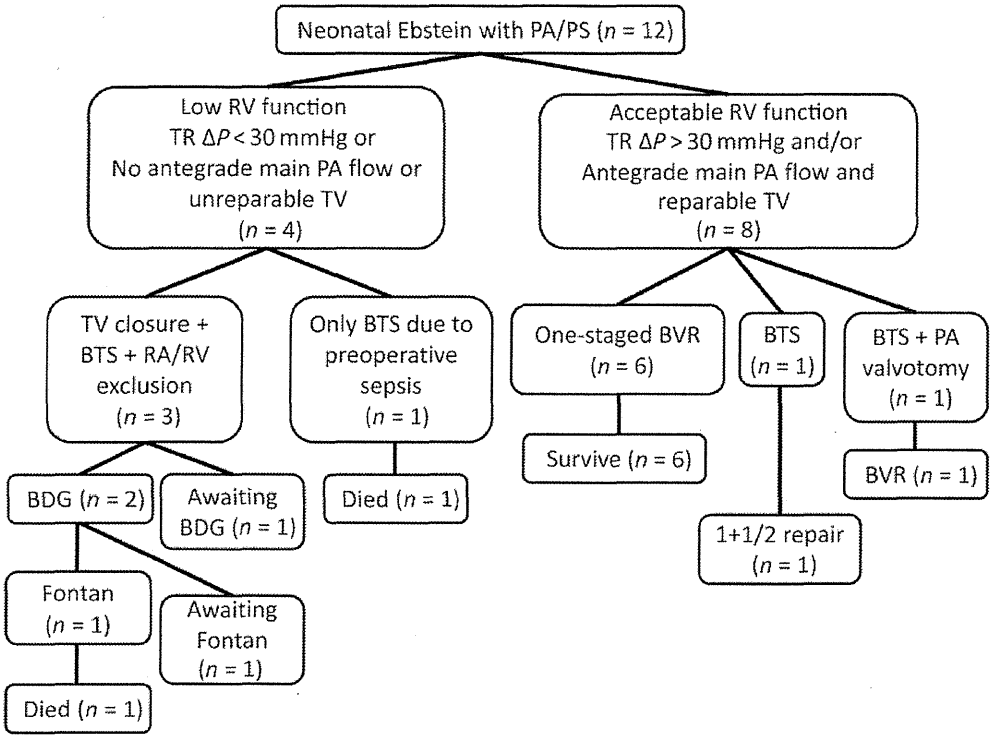

Figure 5: Flow chart of patients. The presence of a trans-TV systolic pressure difference of >30 mmHg and antegrade main pulmonary blood flow are considered important indicators for good RV function. Patients were considered as candidates for the Fontan operation when the pressure difference was <30 mmHg or the TV was not reparable. Four of the 12 patients were considered as Fontan candidates in the present study. The other 8 patients were considered as candidates for BVR or one-and-a-half repair. All the patients with good RV function survived for a long duration. Among the Fontan candidates, 1 case of early death was noted, whereas 1 suddenly died 3 years after the Fontan operation.

The follow-up period of the 11 early survivors was 6.7 ± 4.6 (range, 0.4–12.2) years. There was 1 case of late death (Patient 9 in Table 1). This patient's age at the first surgical intervention was 50 days; he was born at the gestational age of 40 weeks and had a body weight of 3.15 kg at birth. He had PA-IVS (true pulmonary atresia), a PFO and severe TR. Prostaglandin E1 was administered immediately after birth to open the arterial duct. The trans-TV systolic pressure difference was only 4 mmHg, as detected by echocardiography. Based on these findings, the patient was considered as a Fontan candidate. The application of a 4-mm modified BT shunt with exclusion of the RV and RA free walls, closure of the TV with a fenestration, creation of an ASD and ligation of the arterial duct were performed. He had no serious complications postoperatively and was clinically well. He underwent a bidirectional Glenn (BDG) procedure at the age of 8 months and total cavopulmonary connection (TCPC) at the age of 5 years. His main heart rhythm after the TCPC was a junctional rhythm, but he appeared clinically well. However, he suddenly died probably due to a fatal arrhythmia 3 years after the Fontan operation. The actual estimated survival for all patients was 91% at 1 year and 73% at 10 years.

In the 3 patients who underwent RV/RA exclusion, the paradoxical interventricular septal motion, which was present in all these patients preoperatively, was completely normalized. Postoperatively, the marked left ventricular compression due to RV volume overload at end-diastole was improved, and the LV shape at end-diastole was almost circular in the short-axis view—the D-shaped LV observed at end-diastole preoperatively changed to a circular shape postoperatively. Moreover, a small, banana-shaped RV cavity was observed without thrombosis.

Among the 7 patients who underwent a palliative operation, 2 underwent BVR, 1 underwent a one-and-a-half repair, 1 underwent a Fontan operation and 1 underwent a BDG operation. Thus, the final cardiac status of the early survivors was as follows: underwent BVR, underwent one-and-a-half repair, underwent Fontan operation, awaiting Fontan operation and awaiting BDG in 7 (58%), 1 (8%), 1 (8%), 1 (8%) and 1 patient (8%), respectively. Three of the 7 patients who underwent BVR had true pulmonary atresia.

Of the 10 late survivors, 3 patients experienced significant complications. One patient had severe cardiac failure due to a severe myocardial calcification of unknown origin, is currently under treatment and has not been discharged, 1 required home oxygenation therapy after the BDG and 1 required haemolytic therapy due to thrombo-embolism of the artificial pulmonary valve.

The latest examination of the TR in the eight early survivors who underwent TV repair showed that the condition was not present in 1 patient, trivial to mild in 6 and moderate in 1. The latest CTR was 59 ± 9% (range, 45–70%). The serum B-type natriuretic peptide level of the late survivors at a follow-up period of >1 year ($n = 7$) was 46 ± 28 (range, 12–83) pg/ml.

DISCUSSION

Management of a neonatal symptomatic Ebstein's anomaly is extremely challenging, even in institutions with highly experienced surgeons, and is also controversial. Shinkawa *et al.* [5] reported that the overall survival rate estimated for all neonates undergoing surgical intervention was 66.7% at 1 year, 62.2% at 5 and 10 years and 51.9% at 15 years. Knott-Craig *et al.* [6] reported on a series of 22

symptomatic neonates and young infants who underwent BVR, and observed a 73% hospital survival rate. In our current report, 12 patients underwent surgical intervention with a hospital mortality rate of 8.3%. Five of these 12 patients were neonates. All of these neonates are currently alive, and 3 of the 5 neonates were clinically well for >2 years after their first operation. Our results seem to be comparable with or perhaps an improvement over those of these previous reports.

In the present study, a very high rate of successful BVR and one-and-a-half repair with excellent survival was achieved in this patient population. One of the key factors for achieving successful repair in both cases is an estimation of the potential for RV function. Our current policy is that the possibility of BVR should not be excluded at the time of the initial operation in cases where echocardiography indicates a preserved RV function. In the present report, the presence of a trans-TV systolic pressure difference of >30 mmHg, an antegrade main pulmonary blood flow and a good non-atrialized RV morphology were considered as indicators of good RV function. If the patient had pulmonary atresia and a very small trans-TV systolic pressure difference, BVR or one-and-a-half repair was not considered to be feasible, as we believe that no potential for good RV function was present. TV closure and RV/RA exclusion or RV exclusion with RA plication has been selected in Okayama University Hospital for such patients. In other cases where one of the above-mentioned indicators is present and the TV is repairable, we perform a one-stage BVR or TV repair with a BT shunt and the creation of an RV outflow tract as an initial operation.

The feasibility of TV repair is another important factor for performing BVR or one-and-a-half repair. However, it is largely dependent on the surgeon's skill. If a patient has a sail-like anterior leaflet, a conventional tricuspid repair such as Carpentier's repair or Danielson's repair is feasible. However, in other cases, it may not be feasible to repair the TV in such a manner. In the present study, 2 patients had a dysplastic anterior leaflet. One patient (having a mildly dysplastic anterior leaflet) underwent a Cone's operation, whereas the other patient (having a moderately dysplastic anterior leaflet) underwent extensions of the septal and posterior tricuspid leaflets. The postoperative TRs were mild after the operations in both of these patients. Although these operations require a substantial amount of skill, attempting them is valuable because of the outcomes that can be achieved.

A severely enlarged RV compresses the LV and causes abnormal motion of the interventricular septum, which can affect LV function. We have used the total RV/RA exclusion procedure in adults with isolated congestive right heart failure since 1998 and have applied this procedure to patients with severe Ebstein's anomaly since 1999 [4, 7, 8]. This procedure is composed of the resection of the RV free wall, resection or plication of the RA and a cavopulmonary connection or application of a systemic-pulmonary shunt. This procedure increases the volume at end-diastole, restores the cylindrical shape and improves contractile function of the surgically created single LV [7]. The resultant increase in systemic output leads to rapid improvements in the patient's' postoperative condition. The Starnes operation is a simpler procedure and can achieve a comparable effect with regard to LV function improvement when compared with our modified technique, along with normalization of paradoxical interventricular septum motion. However, we believe that a remnant large RV can affect the LV function and have a greater thrombogenic effect when compared with a smaller RV. Further detailed evaluation of postoperative LV function and incidence of postoperative thrombo-embolic events is required to compare postoperative LV function between Starnes operation and our modification. Furthermore, significant lung compression due to an extremely enlarged RA and RV has been reported to be an important risk factor in the survival of neonates with Ebstein's anomaly. Therefore, we believe that RV/RA exclusion is beneficial for postoperative respiratory function and can thus improve postoperative survival [9]. Kajihara *et al.* [10] reported a case of successful management using a 'rapid two-stage Starnes procedure' in neonates with severe Ebstein's anomaly. This group performed main PA ligation, plication of the RA and RV wall, application of a BT shunt and PDA ligation without CPB as an initial operation on the day of birth in order to achieve early lung expansion and improvement in LV function. They subsequently performed Starnes operation using CPB at the age of 12 days. In this previous report, the concept of achieving an early reduction of the enlarged RV and RA to improve LV function and lung function is similar to that in the present study. However, compared with their procedure, the present procedure requires fewer suture lines on the RV than RV plication and requires only 1 surgical intervention. However, the advantages of their surgical strategy include the possibility of reduction of the RV and RA volume while avoiding the risk associated with CPB in the very early neonatal period. Further investigation is required to elucidate the advantages and disadvantages of each surgical strategy for the treatment of neonates with severe Ebstein's anomaly who are not suitable for BVR.

If a patient has a low PA resistance, good LV function and sufficient RV function to handle venous blood volume from the inferior vena cava, the use of one-and-a-half repair could yield good mid-to-long-term results without the occurrence of typical Fontan complications, such as protein-losing enteropathy and congestive liver dysfunction [11]. Therefore, one-and-a-half repair is currently one of the choices for definitive repair at our institution.

The major limitation of this study is the small number of patients. All patients were treated with the same strategy in the present study. Therefore, we were unable to perform comparisons between patients who underwent an RV exclusion procedure and those who did not undergo this procedure for verifying the effect of the RV exclusion procedure on postoperative LV function. Thus, further accumulation of surgical experiences and investigation on the real benefits of RV/RA exclusion are required.

CONCLUSIONS

Critically ill neonates and small infants with Ebstein's anomaly and poor RV function can be successfully treated by RV/RA exclusion or RV exclusion with RA plication in addition to BT shunt application. However, in cases with good RV function, primary BVR is advocated. Our management strategy for neonates with symptomatic Ebstein's anomalies was beneficial for avoiding a future establishment of Fontan circulation. Cone reconstruction and reconstruction of the septal and posterior leaflets were good options for increasing the likelihood of successful TV repair.

Conflict of interest: none declared.

REFERENCES

[1] Boston US, Goldberg SP, Ward KE, Overholt ED, Spentzas T, Chin TK *et al.* Complete repair of Ebstein anomaly in neonates and young infants: a 16-year follow-up. J Thorac Cardiovasc Surg 2011;141:1163–9.

[2] Bove EL, Hirsch JC, Ohye RG, Devaney EJ. How I manage neonatal Ebstein's anomaly. Semin Thorac Cardiovasc Surg Pediatr Card Surg Annu 2009;12:63–5.
[3] Starnes VA, Pitlick PT, Bernstein D, Griffin ML, Choy M, Shumway NE. Ebstein's anomaly appearing in the neonate. A new surgical approach. J Thorac Cardiovasc Surg 1991;101:1082–7.
[4] Sano S, Ishino K, Kawada M, Kasahara S, Kohmoto T, Takeuchi M *et al.* Total right ventricular exclusion procedure: an operation for isolated congestive right ventricular failure. J Thorac Cardiovasc Surg 2002;123:640–7.
[5] Shinkawa T, Polimenakos AC, Gomez-Fifer CA, Charpie JR, Hirsch JC, Devaney EJ *et al.* Management and long-term outcome of neonatal Ebstein anomaly. J Thorac Cardiovasc Surg 2010;139:354–8.
[6] Knott-Craig CJ, Goldberg SP, Overholt ED, Colvin EV, Kirklin JK. Repair of neonates and young infants with Ebstein's anomaly and related disorders. Ann Thorac Surg 2007;84:587–92.
[7] Takagaki M, Ishino K, Kawada M, Otsuki SI, Hirota M, Tedoriya T *et al.* Total right ventricular exclusion improves left ventricular function in patients with end-stage congestive right ventricular failure. Circulation 2003;108 (Suppl 1):II-226–9.
[8] Kawabata T, Kasahara S, Arai S, Sano S. Right ventricular exclusion for a neonatal patient with Ebstein anomaly: a free wall resection of the right ventricle. J Thorac Cardiovasc Surg 2011;142:1582–4.
[9] Tanaka T, Yamaki S, Ohno T, Ozawa A, Kakizawa H, Iinuma K. The histology of the lung in neonates with tricuspid valve disease and gross cardiomegaly due to severe regurgitation. Pediatr Cardiol 1998;19:133–8.
[10] Kajihara N, Asou T, Takeda Y, Kosaka Y, Onakatomi Y, Miyata D *et al.* Rapid two-stage Starnes procedure for a symptomatic neonate with Ebstein anomaly. Ann Thorac Surg 2010;90:2073–5.
[11] Kim S, Al-Radi O, Friedberg MK, Caldarone CA, Coles JG, Oechslin E *et al.* Superior vena cava to pulmonary artery anastomosis as an adjunct to biventricular repair: 38-year follow-up. Ann Thorac Surg 2009;87:1475–82.

APPENDIX. CONFERENCE DISCUSSION

***Dr O. Ghez** (London, UK)*: Your study reflects very well the challenging management of children with this malformation. Clearly the treatment must be tailored to each individual patient, as you showed very well in your 12 patients, who all had different operations. You emphasize in your manuscript that even though the procedure of RV exclusion, which you already described, provides excellent haemodynamic results for univentricular palliation, some children can be saved towards a biventricular repair in this selected group of symptomatic neonates. Your criteria for primary repair are a well functioning right ventricle, which is not so easy to assess, as you showed, and a repairable tricuspid valve, about which maybe you could elaborate a bit more. With your strategy, you achieved excellent results in these 12 patients, with only one early death and one late death. I noticed, however, that three of your patients did not go into this route of either RV exclusion or biventricular repair immediately. Three of those had a BT shunt and then eventually two of those went to a biventricular repair and one to a one and a half ventricular repair.

Regarding the first operation, can I ask you to clarify your indications for performing a systemic to pulmonary artery shunt, either isolated or associated with an RVOT opening? This is not very clear in the manuscript. In other words, when would you stage a repair in these patients? This is my first question.

And the last question, you used several techniques for tricuspid valve repair in the four patients in whom it was performed. One of those had a cone repair. Is it now your treatment of choice?

Dr Sano: In response to your first question, the indication for the modified BT shunt alone is in the patients who have less than moderate tricuspid regurgitation, and also the patients with a CTR less than 80%, as well as in the patients where their future indication is possibly biventricular repair.

The indication for the modified BT shunt with RV outflow tract reconstruction, is in the patients who have rather good RV function and also the patients who may be candidates for future biventricular repair. If the patients have very bad RV function or a very thin RV wall, regurgitation increases from the pulmonary artery to the RV if pulmonary valvotomy or RV outflow tract reconstruction is performed. Finally, the RV distends and these patients do not do well.

Indications for RV/RA exclusion is in patients who have a huge CTR, >90%, severe tricuspid regurgitation and poor RV function. It is not always easy to evaluate the RV function in the neonatal period, so one of these patients achieved a one and a half ventricular repair later on. For patients in the initial palliation group, the second stage operation should be done at around six to 12 months, if possible, certainly at older than three months, because a bidirectional Glenn procedure can be done.

Your final question relates to my recent preference for tricuspid valve repair. I now do more cone operations in older patients, and I am very happy with the results. Recently, I tried to use the cone operation in the neonate. I did only one cone operation in my university, and I did another one in the other unit.

***Dr J. Amato** (Chicago, IL, USA)*: I just wanted to pinpoint the one patient in whom you had the plication. I am a little surprised, because I had a little bit more in my series, but what was your technique for the plication and what did you do with the valve adjacent to that plication?

Dr Sano: In that particular patient it was a little bit dangerous to repair under cardiopulmonary bypass, so I did a shunt, and a suture to the right atrium to make the right atrium small.

Dr Amato: Did you have to do anything to that leaflet of the valve in the plication?

Dr Sano: No. In the second stage I did. In the first stage I did a BT shunt and an RV plication to the surface without using bypass.

***Dr M. Wojtalik** (Poznan, Poland)*: According to your presentation, after right ventricular resection you close the tricuspid valve. Do you think it is always necessary in all cases for such an operation?

Dr Sano: I presented the abnormal interventricular septal motion (IVS) at the STS meeting. The IVS motion is abnormal in these patients because the huge dilated RV compresses the LV. However, the abnormal motion disappears after surgery because the dilated RV becomes small. I showed the video of the patient with more than 400% of normal size RV. In the patient whose RV is 200 or 250% of normal and in whom the IVS motion is not paradoxical, RV exclusion is not performed. It is not always necessary to do RV/RA exclusion. Only the patients who had a huge dilated RV which compressed the LV were selected for RV exclusion. Soon after the operation the LV becomes bigger, because IVS shifts to the RV side and LV shape returns to normal, therefore LV stroke volume increases and ejection fraction improves.

Dr Wojtalik: But after exclusion do you always close the tricuspid valve?

Dr Sano: Most of these patients had severe tricuspid regurgitation, a huge RV, and a very thin RV wall, so I did exclude the RV/RA. But some of the patients who had a 200–300% of normal size RV with rather good RV function, had plication or exclusion of RA and repair of the tricuspid valve without exclusion of the RV.

Life Sciences 114 (2014) 102–106

Contents lists available at ScienceDirect

Life Sciences

journal homepage: www.elsevier.com/locate/lifescie

Effects of intravenous cariporide on release of norepinephrine and myoglobin during myocardial ischemia/reperfusion in rabbits

Shigeru Sakurai [a], Yosuke Kuroko [a], Shuji Shimizu [a,b,*], Toru Kawada [b], Tsuyoshi Akiyama [c], Toji Yamazaki [d], Masaru Sugimachi [b], Shunji Sano [a]

[a] Department of Cardiovascular Surgery, Okayama University Graduate School of Medicine, Dentistry and Pharmaceutical Sciences, Okayama 700-8558, Japan
[b] Department of Cardiovascular Dynamics, National Cerebral and Cardiovascular Center, Osaka 565-8565, Japan
[c] Department of Cardiac Physiology, National Cerebral and Cardiovascular Center, Osaka 565-8565, Japan
[d] Department of Anesthesiology, National Hospital Organization Kinki-Chuo Chest Medical Center, Osaka 591-8555, Japan

ARTICLE INFO

Article history:
Received 12 May 2014
Accepted 8 August 2014
Available online 17 August 2014

Keywords:
Cariporide
Myoglobin
Norepinephrine
Ischemia/reperfusion

ABSTRACT

Aims: To examine the effects of cariporide, a Na^+/H^+ exchanger-1 inhibitor, on cardiac norepinephrine (NE) and myoglobin release during myocardial ischemia/reperfusion by applying a microdialysis technique to the rabbit heart.

Main methods: In anesthetized rabbits, two dialysis probes were implanted into the left ventricular myocardium and were perfused with Ringer's solution. Cariporide (0.3 mg/kg) was injected intravenously, followed by occlusion of the left circumflex coronary artery. During 30-min coronary occlusion followed by 30-min reperfusion, four consecutive 15-min dialysate samples (two during ischemia and two during reperfusion) were collected in vehicle and cariporide-treated groups. Dialysate myoglobin and NE concentrations were measured by immunochemistry and high-performance liquid chromatography, respectively.

Key findings: Dialysate myoglobin and NE concentrations increased significantly during myocardial ischemia/reperfusion in both vehicle and cariporide-treated groups ($P < 0.01$ vs. baseline). In cariporide-treated group, dialysate myoglobin concentrations were significantly lower than those in vehicle group throughout ischemia/reperfusion ($P < 0.01$ at 0–15 min of ischemia, $P < 0.05$ at 15–30 min of ischemia, $P < 0.01$ at 0–15 min of reperfusion, and $P < 0.01$ at 15–30 min of reperfusion). However, dialysate NE concentrations in cariporide-treated group were lower than those in vehicle group only during ischemia ($P < 0.01$ at 0–15 min of ischemia, and $P < 0.05$ at 15–30 min of ischemia).

Significance: When administered before ischemia, cariporide reduces myoglobin release during ischemia/reperfusion and decreases NE release during ischemia.

Introduction

The Na^+/H^+ exchanger isoform-1 (NHE-1) is a ubiquitously expressed integral membrane protein transporter that regulates intracellular pH by removing intracellular H^+ in exchange for extracellular Na^+ (Fliegel, 2005). NHE-1 has been reported to play an important role in the pathogenesis of myocardial ischemia/reperfusion injuries (Avkiran, 1999, 2003). During myocardial ischemia/reperfusion, the activity or quantity of NHE-1 increases, leading to an accumulation of intracellular Na^+, which in turn reduces and eventually reverses the driving force for the Na^+/Ca^{2+} exchanger, thereby decreasing Ca^{2+} efflux and eventually increasing Ca^{2+} influx. This process subsequently induces intracellular Ca^{2+} overload and promotes structural (apoptosis) and functional (arrhythmias, hypercontraction) damages (Leineweber et al., 2007). In sympathetic nerve endings, increased NHE-1 activity results in accumulation of axoplasmic Na^+ that diminishes the inward transport and eventually favors the outward transport of norepinephrine (NE) via the neuronal NE transporter (a bidirectional NE carrier, NET) (Leineweber et al., 2007). Thus, inhibition of NHE-1 may reduce NE release into the synaptic cleft. Because excessive NE release from sympathetic nerve endings is a prominent cause of arrhythmias and cardiac dysfunction (Leineweber et al., 2007), NHE-1 inhibitors may provide cardioprotection against functional damage during ischemia/reperfusion.

Cariporide, a NHE-1 inhibitor, has been reported to be a pharmacologically preconditioning agent. Several experimental studies have demonstrated that pretreatment with cariporide reduces infarct size (Kristo et al., 2004; Miura et al., 1997), suggesting that the inhibition of NHE-1 protects the heart from structural damage during ischemia/reperfusion. Furthermore, Létienne et al. (2006) reported that cariporide significantly reduced plasma myoglobin and troponin I

* Corresponding author at: Department of Cardiovascular Dynamics, National Cerebral and Cardiovascular Center, 5-7-1 Fujishiro-dai, Suita, Osaka 565-8565, Japan. Tel.: +81 6 6833 5012; fax: +81 6 6835 5403.
E-mail address: shujismz@ri.ncvc.go.jp (S. Shimizu).

http://dx.doi.org/10.1016/j.lfs.2014.08.008
0024-3205/

levels that strongly correlated with myocardial necrosis. Therefore, cariporide treatment before ischemia may reduce both pathological NE release and structural damage of the heart during ischemia/reperfusion. However, because of the limited methodology for simultaneous monitoring NE release and structural heart damage in the past, the mechanism of cardioprotection by cariporide has not been fully elucidated. Our group has already demonstrated that cardiac microdialysis technique can simultaneously monitor interstitial NE and myoglobin levels in the ischemic region of the left ventricle (Kitagawa et al., 2005). Because there is less blood flow in ischemic lesion, diffusion of myoglobin should be limited. Therefore interstitial myoglobin level monitored by cardiac microdialysis technique may serve as a more accurate index of structural damage of the heart than plasma myoglobin level. Using this technique, we investigated the effects of cariporide on both NE and myoglobin releases in the left ventricle during ischemia/reperfusion.

Materials and methods

Animal preparation

Animal care was provided in accordance with the *Guiding Principles for the Care and Use of Animals in the Field of Physiological Sciences* approved by the Physiological Society of Japan. All protocols were approved by the Animal Subject Committee of the National Cerebral and Cardiovascular Center. Twelve adult male Japanese white rabbits weighing from 2.5 to 3.5 kg were anesthetized with an intravenous injection of pentobarbital sodium (40 mg/kg) via the marginal ear vein, followed by continuous intravenous infusion of pentobarbital sodium (2 mg/kg/h). Butorphanol (0.1 mg/kg) was injected intramuscularly every 2–3 h for analgesia. Adequate anesthesia level was confirmed by loss of the ear pinch response. The rabbits were intubated and ventilated mechanically with room air mixed with oxygen. Systemic arterial pressure was monitored by a catheter inserted into the femoral artery. Heparin sodium (10 IU/kg/h) was infused to prevent blood coagulation in the femoral artery catheter. Heart rate was monitored on body surface electrocardiogram. Arterial pressure and heart rate were recorded by a PowerLab Data Acquisition System (ADInstruments, Dunedin, New Zealand). Esophageal temperature was maintained between 38 and 39 °C using a heating pad.

With the animal in the lateral position, the fifth or sixth rib on the left side was partially removed and a small incision was made in the pericardium to expose the heart. A snare was placed around the main branch of the left circumflex coronary artery (LCX) to act as an occluder for later coronary occlusion. Two dialysis probes were implanted in the left ventricular wall corresponding to the region perfused by the LCX. To confirm that the dialysis probes were properly located inside the ischemic region, we examined the color and motion of the ventricular wall during a brief occlusion. To avoid a preconditioning effect, the duration of brief occlusion was limited to a few seconds.

At the end of each experiment, the LCX was again occluded. Evans blue (1%) was intravenously injected to confirm that the dialysis probes were properly implanted within the ischemic area. The rabbits were euthanized by injecting an overdose of pentobarbital sodium. At postmortem, the heart was excised from the euthanized rabbit and was transversely sliced into 3 or 4 pieces. The left ventricular cavity was macroscopically examined to confirm that the dialysis membranes were not exposed to the left ventricular cavity.

Dialysis technique

Materials for cardiac microdialysis probe have been described in detail previously (Akiyama et al., 1991; Kitagawa et al., 2005). The long transverse dialysis probes were custom made. For monitoring myocardial interstitial NE levels, a dialysis fiber (length 8 mm, o.d. 0.31 mm, i.d. 0.20 mm; PAN-1200 50,000 molecular weight cutoff; Asahi Chemical Japan) was glued at both ends to polyethylene tubes. This dialysis probe was perfused with Ringer's solution at a rate of 2 μl/min using a microinjection pump (Carnegie Medicine CMA/102, Sweden). Each dialysate sample was collected over 15 min (1 sampling volume = 30 μl) into a microtube containing 3 μl of 0.1 N HCl to prevent amine oxidation. Dialysate NE level was measured by high-performance liquid chromatography with electrochemical detection (ECD-300, Eicom, Japan) as described in the Analytical procedures section.

For monitoring myocardial interstitial myoglobin levels, another dialysis probe (length 8 mm, o.d. 0.215 mm, i.d. 0.175 mm, 300 Å pore size; Evaflux type 5A; Kuraray Medical, Japan) was used as described previously (Kitagawa et al., 2005). This dialysis probe was perfused with Ringer's solution at a rate of 5 μl/min. Dialysate sampling period was 15 min (1 sampling volume = 75 μl). Dialysate myoglobin concentration was measured by immunochemistry using a Cardiac Reader (Roche Diagnostics, Basel, Switzerland) as described in the Analytical procedures section.

Experimental protocols were started 2 h after implantation of the dialysis probes. During dialysate sampling, we took into account the dead space between the dialysis membrane and the sample tube.

Analytical procedures

Dialysate NE concentrations were measured by high-performance liquid chromatography with electrochemical detection. An alumina procedure was employed to remove the interfering compounds from the dialysate samples. The liquid chromatography system consisted of a pump (EP-300, Eicom) with a degasser (DG-300, Eicom), a separation column (Eicompak CA-5ODS, Eicom), and an electrochemical detector (ECD-300, Eicom). The temperature of the separation was maintained at 25 °C by a column oven (ATC-300, Eicom). The electrochemical detector was operated with a graphite electrode (WE-3G, Eicom) at +0.45 V vs. an Ag/AgCl reference electrode. Mobile phase consisted of 12% (v/v) methanol, 1-octanesulfonic acid sodium (600 mg/l) and 88% (v/v) 100-mM phosphate buffer adjusted to pH 5.68. The pump flow rate was 0.23 ml/min. Chromatograms were recorded and analyzed by a laboratory computer connected with an A–D converter (Power Chrom EPC-500, Eicom). NE concentrations were determined by measuring the peak areas. The absolute detection limit of NE was 0.1 pg per injection (signal-to-noise ratio = 3).

Dialysate myoglobin concentrations were measured by the Cardiac Reader system (Roche Diagnostics). Single-use immunochemical test strips were used in the Cardiac Reader system. When a sample was added to the test well, the sample migrated along the strip due to capillary action, and myoglobin combined with two specific monoclonal antibodies. The resulting sandwich complex was immobilized by streptavidin in a stripe along the read window, producing a reddish line with an intensity related to myoglobin concentration. The CCD (Charge Coupled Device) camera quantified the intensity of the signal line and control line on the immunochemical test strips via reflectance measurements. The reflectance measurements were then converted into myoglobin concentration using electronically stored lot-specific calibration curves. The measuring range was between 30 and 700 ng/ml (Ambrose et al. 2002). When dialysate myoglobin concentrations were expected to be higher than 700 ng/ml, dialysate samples were diluted 10 or 100 times with saline.

Experimental protocols

Time courses of dialysate NE and myoglobin concentrations during acute myocardial ischemia/reperfusion (n = 6, vehicle group)

We examined the time courses of dialysate NE and myoglobin concentrations during 30 min of ischemia followed by 30 min of reperfusion. After 15-min baseline sampling, the main branch of the LCX was occluded for 30 min and then was released. Four consecutive 15-min

dialysate samples were collected during coronary occlusion (30 min) and reperfusion (30 min).

Influence of cariporide on time courses of dialysate NE and myoglobin concentrations during acute myocardial ischemia/reperfusion (n = 6, cariporide-treated group)

We examined the effects of cariporide on NE and myoglobin releases during ischemia/reperfusion. Ten-mg powder of cariporide (Santa Cruz Biotechnology, Inc., CA, USA) was dissolved in 10-ml saline. After 15-min baseline sampling, cariporide of 0.3 mg/kg, which reportedly caused a sufficient reduction in infarct mass (Linz et al., 1998), was injected intravenously before coronary occlusion. The LCX occlusion and reperfusion were performed as described in the vehicle group, and four consecutive dialysate samples were collected.

Statistical methods

All data are presented as mean ± standard error. For each protocol, heart rate and mean arterial pressure were compared by one-way repeated measures analysis of variance followed by a Dunnett's test versus baseline. After logarithmic transformation, dialysate NE and myoglobin concentrations were compared by one-way repeated measures analysis of variance followed by a Dunnett's test versus baseline. The differences between two groups were compared by unpaired *t*-test. Statistical significance was defined as $P < 0.05$.

Results

Time courses of heart rate and mean arterial pressure

The time courses of heart rate and mean arterial pressure during myocardial ischemia/reperfusion are shown in Table 1. In the vehicle group, coronary occlusion did not affect heart rate or mean arterial pressure. After reperfusion, heart rate decreased significantly but slightly to 266 ± 6 bpm at 7.5 min (compared with baseline: 277 ± 5 bpm; $P < 0.05$) and 265 ± 4 bpm at 22.5 min of reperfusion ($P < 0.05$ vs. baseline). In the cariporide-treated group, heart rate and mean arterial pressure did not change throughout ischemia and reperfusion.

There were no significant differences between the vehicle and cariporide-treated groups in heart rate and mean arterial pressure throughout the experiment.

Time course of dialysate NE concentration

Time course of dialysate NE concentration is shown in Fig. 1. In some baseline samples, dialysate NE concentrations were below the detection limit (0.1 pg/30-μl injection). For statistical analysis, baseline values were represented by the detection limit of 3.7 pg/ml.

In the vehicle group, dialysate NE concentration increased to 7251 ± 1891 pg/ml at 0–15 min of ischemia ($P < 0.01$ vs. baseline), reaching a peak of 56,586 ± 10,972 pg/ml at 15–30 min of ischemia ($P < 0.01$ vs. baseline). After reperfusion, dialysate NE concentration decreased to 16,837 ± 3906 pg/ml at 0–15 min ($P < 0.01$ vs. baseline), and further to 675 ± 243 pg/ml at 15–30 min of reperfusion ($P < 0.01$ vs. baseline).

In the cariporide-treated group, dialysate NE concentration increased significantly to 1174 ± 273 pg/ml at 0–15 min of ischemia ($P < 0.01$ vs. baseline), reaching a peak of 29,278 ± 4138 pg/ml at 15–30 of ischemia ($P < 0.01$ vs. baseline). After reperfusion, dialysate NE concentration decreased to 11,913 ± 3145 pg/ml at 0–15 min ($P < 0.01$ vs. baseline), and further to 414 ± 133 pg/ml at 15–30 min of reperfusion ($P < 0.01$ vs. baseline).

Dialysate NE concentrations in the cariporide-treated group were significantly lower than those in the vehicle group during ischemia ($P < 0.01$ at 0–15 min and $P < 0.05$ at 15–30 min). However, there were no significant differences in dialysate NE concentration between two groups during reperfusion.

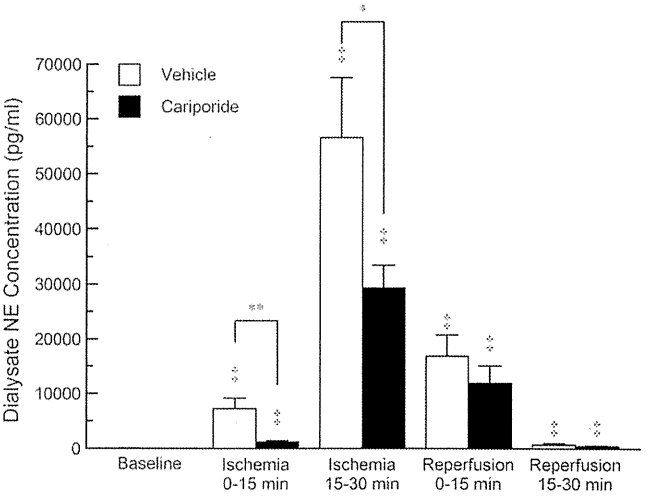

Fig. 1. Time courses of dialysate norepinephrine (NE) concentration during 30 min of ischemia followed by 30 min of reperfusion. Each dialysate sample was collected over a period of 15 min. Data are expressed as mean ± standard error. ‡$P < 0.01$, by ANOVA followed by Dunnett's test versus baseline; *$P < 0.05$ and **$P < 0.01$, by unpaired *t*-test.

Table 1
Heart rate and mean arterial pressure during acute myocardial ischemia/reperfusion.

	Baseline	Ischemia 7.5 min	Ischemia 22.5 min	Reperfusion 7.5 min	Reperfusion 22.5 min
Vehicle (n = 6)					
Heart rate (bpm)	277 ± 5	269 ± 6	267 ± 4	266 ± 6*	265 ± 4*
Mean arterial pressure (mm Hg)	84 ± 4	80 ± 5	82 ± 5	82 ± 6	82 ± 6
Cariporide (n = 6)					
Heart rate (bpm)	274 ± 4	278 ± 6	276 ± 5	271 ± 6	269 ± 3
Mean arterial pressure (mm Hg)	80 ± 2	85 ± 3	85 ± 3	78 ± 2	75 ± 1

Data are expressed as mean ± standard error. *$P < 0.05$ by ANOVA followed by Dunnett's test versus baseline.

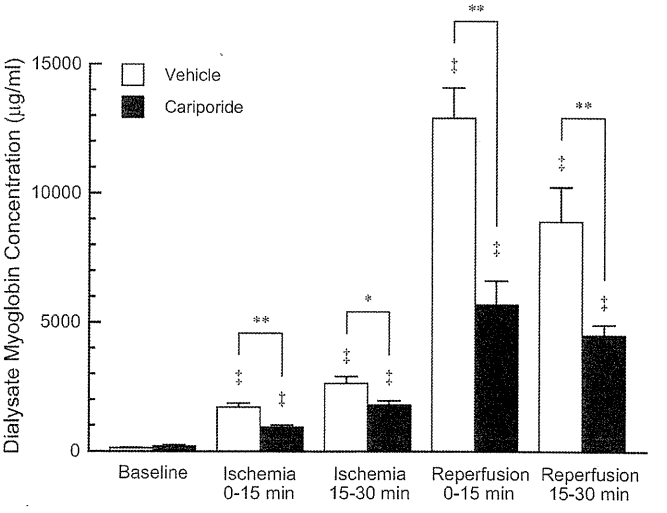

Fig. 2. Time courses of dialysate myoglobin concentration during 30 min of ischemia followed by 30 min of reperfusion. Each dialysate sample was collected over a period of 15 min. Data are expressed as mean ± standard error. ‡$P < 0.01$, ANOVA followed by Dunnett's test versus baseline; *$P < 0.05$ and **$P < 0.01$, by unpaired t test.

Time course of dialysate myoglobin concentration

Time course of dialysate myoglobin concentration is shown in Fig. 2. In the vehicle group, dialysate myoglobin concentration increased significantly from 128 ± 25 ng/ml at baseline to 1717 ± 137 ng/ml at 0–15 min of ischemia ($P < 0.01$ vs. baseline), and further to 2630 ± 262 ng/ml at 15–30 min of ischemia ($P < 0.01$ vs. baseline). After reperfusion, dialysate myoglobin concentration reached a peak of 12,887 ± 1186 ng/ml at 0–15 min ($P < 0.01$ vs. baseline), followed by a gradual decline (8903 ± 1317 ng/ml at 15–30 of after reperfusion, $P < 0.01$ vs. baseline).

In the cariporide-treated group, dialysate myoglobin concentration increased significantly from 218 ± 38 ng/ml at baseline to 943 ± 80 ng/ml at 0–15 min of ischemia ($P < 0.01$ vs. baseline), and further to 1798 ± 169 ng/ml at 15–30 min of ischemia ($P < 0.01$ vs. baseline). After reperfusion, dialysate myoglobin concentration reached a peak of 5690 ± 924 ng/ml at 0–15 min ($P < 0.01$ vs. baseline), followed by a gradual decline (4500 ± 395 ng/ml at 15–30 min of reperfusion, $P < 0.01$ vs. baseline).

Dialysate myoglobin concentrations in the cariporide-treated group were significantly lower than those in the vehicle group throughout ischemia/reperfusion ($P < 0.01$ at 0–15 min of ischemia, $P < 0.05$ at 15–30 min of ischemia, $P < 0.01$ at 0–15 min of reperfusion and $P < 0.01$ at 15–30 min of reperfusion).

Discussion

The present study demonstrated that intravenous injection of cariporide before coronary occlusion significantly reduced interstitial myoglobin levels during ischemia/reperfusion, and suppressed NE release from sympathetic nerve endings during ischemia but not during reperfusion.

NHE-1 inhibition and NE release

During acute myocardial ischemia, excessive NE release from sympathetic nerve endings and reduced NE reuptake into nerve endings may cause functional damages such as life-threatening arrhythmia. There are two major processes of NE release from sympathetic nerve endings. Under physiological conditions, NE is mainly released via Ca^{2+}-dependent exocytosis. In myocardial ischemia, however, the predominant process of NE release is Ca^{2+}-independent nonexocytosis via NET (Kurz et al., 1995). Physiologically, NET relocates NE within the synaptic cleft into the axoplasm, where NE is taken up into storage vesicles or degraded by monoamine oxidase. The NE vesicular storage depends on the pH gradient across the vesicular membrane maintained by an ATP-dependent H^+ pump. Increase in H^+ due to lowered pH as well as ATP depletion during ischemia leads to an increase in free axoplasmic NE (Leineweber et al., 2007), and activates the influx of Na^+ via NHE-1. Since the direction of NET-mediated transport depends on the Na^+ gradient across the membrane of sympathetic nerve terminals (Schömig et al., 1991), a rise in axoplasmic Na^+ concentration during ischemia diminishes the inward transport and favors the outward transport of NE, causing excessive Ca^{2+}-independent nonexocytotic NE release (Leineweber et al., 2007). Thus, by inhibiting NHE-1, cariporide may reduce the influx of Na^+ and suppress nonexocytotic NE release during ischemia. The present study proved that cariporide significantly reduces interstitial NE levels during ischemia. Therefore, cariporide may suppress functional damage caused by excessive NE release during ischemia.

This study also provided important evidence that cariporide does not reduce NE release during reperfusion. Thus, the effects of cariporide against excessive NE release may be limited to the ischemic period but not during reperfusion. This may be a reason why several clinical trials failed to prove the cardioprotective effects of NHE-1 inhibitors administered shortly before reperfusion. In the ESCAMI (Evaluation of the Safety and Cardioprotective Effects of Eniporide in Acute Myocardial Infarction) trial, administration of eniporide before reperfusion in patients with acute myocardial infarction did not improve clinical outcomes (death, cardiogenic shock, heart failure, life-threatening arrhythmias) (Zeymer et al., 2001). A previous study demonstrated that myocardial interstitial NE level decreased while dihydroxyphenylglycol (a metabolite of NE) level increased rapidly after reperfusion (Akiyama and Yamazaki, 2001). Thus, metabolites of catecholamine may also be associated with functional damage during reperfusion. Further investigations are necessary to clarify the effects of NHE-1 inhibitors on functional damage during reperfusion.

NHE-1 inhibition and myoglobin release

During myocardial ischemia, anaerobic glycolysis and ATP degradation produce H^+ that activates the influx of Na^+ via NHE-1. However, Na^+ efflux is attenuated because the Na^+/K^+-ATPase is inhibited during ischemia. Therefore, the net result enhanced Na^+ influx and reduced Na^+ efflux. An accumulation of intracellular Na^+ induces cytoplasmic Ca^{2+} overload via reverse-mode Na^+/Ca^{2+} exchanger, resulting in structural damage during myocardial ischemia/reperfusion (Leineweber et al., 2007). Therefore, cariporide may reduce Na^+ influx and suppress Ca^{2+} overload, resulting in the reduction of structural damage indicated by myoglobin release. Furthermore, several possible mechanisms of cardioprotective effects of cariporide have already been suggested. Nuñez et al. (2011) reported that attenuation of calcium-induced permeability transition pore opening after protein kinase C (PKC)-mediated mitochondrial ATP-sensitive potassium channel activation was a crucial step for the cardioprotective effects of cariporide. On the other hand, Ajiro et al. (2011) reported that platelet-activating factor (PAF) stimulated cardiac NHE-1 via the PAF receptor and signal relay required participation of the mitogen-activated protein kinase cascade. They also reported that PKC might not be involved in the stimulation of NHE-1 because PKC inhibitors did not significantly reduce the responses to PAF. Further investigations are clearly needed to identify the mechanisms.

Létienne et al. (2006) reported that cariporide significantly reduced plasma myoglobin level that strongly correlated with myocardial necrosis. However, we have previously demonstrated that plasma myoglobin level responds less sensitively than myocardial interstitial myoglobin level monitored by cardiac microdialysis (Kitagawa et al., 2005). Although a significant change in plasma myoglobin level occurs at 45–60 min after coronary occlusion in a rabbit ischemia model (Kitagawa et al., 2005), the myocardial microdialysis technique can detect a significant change in interstitial myoglobin level within 15 min after occlusion. The present study demonstrated that cariporide reduced interstitial myoglobin level from the early phase (0–15 min) of myocardial ischemia and this effect was sustained even after reperfusion was started. Several experimental studies have reported that preconditioning with cariporide salvages myocytes and reduces the release of cardiac-specific enzymes (Cun et al., 2007; Haist et al., 2003). Furthermore, the GUARDIAN (Guard During Ischemia Against Necrosis) trial revealed a significant correlation between elevated creatine kinase myocardial band (CK-MB) during the initial 48 h after coronary artery bypass grafting (CABG) and significantly increased six-month mortality (Gavard et al., 2003). A subgroup analysis of the GUARDIAN data revealed that a 120-mg dose of cariporide significantly reduced the combined incidence of death and myocardial infarction in patients undergoing high-risk CABG surgery, and that this benefit was sustained for 6 months (Boyce et al., 2003). Therefore, a reduction in the release of cardiac enzymes after reperfusion may have a close relation to the improvement of surgical outcomes. In the present study, cariporide also suppressed peak interstitial myoglobin level after reperfusion. Thus, cariporide administration before ischemia may be an effective cardioprotective strategy against structural damage during ischemia/reperfusion.

On the other hand, several studies have demonstrated that treatment with cariporide shortly before reperfusion does not

reduce infarct size (Miura et al., 1997; Reffelmann and Kloner, 2003). Klein et al. (2000) reported that the reduction of infarct size was detectable only when cariporide was infused during the first 30 min after ischemia. In their study, cariporide infused after 45 min of ischemia until 10 min of reperfusion failed to reduce infarct size. In the ESCAMI trial, pretreatment with eniporide in patients undergoing reperfusion therapy for acute ST-elevation myocardial infarction did not reduce infarct size assessed by cardiac enzyme release (Zeymer et al., 2001). The present study revealed that pretreated cariporide significantly reduced interstitial myoglobin level from the very early phase after myocardial ischemia. This fact may be a reason why cariporide should be administered before ischemia to exert its cardioprotective effects. Thus, the reduction of interstitial myoglobin level during reperfusion observed in the present study may reflect amelioration of structural damage caused by ischemia and not necessarily the damage induced by reperfusion. Nevertheless, cariporide has a certain cardioprotective effect against structural damage during ischemia and reperfusion.

Methodological considerations

The responses of heart rate and arterial pressure to myocardial ischemia/reperfusion were small in the present study. Because Kashihara et al. (2004) reported that Bezold–Jarisch (B–J) reflex induced by phenylbiguanide blunted arterial baroreflex via the shift of the neural arc toward lower sympathetic nerve activity, small responses in heart rate and arterial pressure might be due to weak B–J reflex during acute myocardial ischemia in rabbits.

Conclusions

Intravenous cariporide significantly reduced myocardial interstitial myoglobin level during ischemia/reperfusion and decreased NE release during ischemia. When administered before ischemia, treatment with cariporide may be an effective cardioprotective strategy against structural damage during ischemia/reperfusion and excessive NE release during ischemia.

Conflict of interest statement

The authors declare that there are no conflicts of interest.

Acknowledgment

This study was supported by a Medical Research Promotion Grant from the Takeda Science Foundation, Japan.

References

Ajiro Y, Saegusa N, Giles WR, Stafforini DM, Spitzer KW. Platelet-activating factor stimulates sodium–hydrogen exchange in ventricular myocytes. Am J Physiol Heart Circ Physiol 2011;301:H2395–401.

Akiyama T, Yamazaki T. Myocardial interstitial norepinephrine and dihydroxyphenylglycol levels during ischemia and reperfusion. Cardiovasc Res 2001;49:78–85.

Akiyama T, Yamazaki T, Ninomiya I. In vivo monitoring of myocardial interstitial norepinephrine by dialysis technique. Am J Physiol 1991;261:H1643–7.

Ambrose TM, Knight D, Neher J. The Cardiac Reader: A Platform for Quantitative Point-of-Care Cardiac Marker Determinations From Roche Diagnostics. Point of Care. 2002;1:50–3.

Avkiran M. Rational basis for use of sodium–hydrogen exchange inhibitors in myocardial ischemia. Am J Cardiol 1999;83:10C–7C.

Avkiran M. Basic biology and pharmacology of the cardiac sarcolemmal sodium/hydrogen exchanger. J Card Surg 2003;18(Suppl. 1):3–12.

Boyce SW, Bartels C, Bolli R, Chaitman B, Chen JC, Chi E, et al. Impact of sodium–hydrogen exchange inhibition by cariporide on death or myocardial infarction in high-risk CABG surgery patients: results of the CABG surgery cohort of the GUARDIAN study. J Thorac Cardiovasc Surg 2003;126:420–7.

Cun L, Ronghua Z, Bin L, Jin L, Shuyi L. Preconditioning with Na^+/H^+ exchange inhibitor HOE642 reduces calcium overload and exhibits marked protection on immature rabbit hearts. ASAIO J 2007;53:762–5.

Fliegel L. The Na^+/H^+ exchanger isoform 1. Int J Biochem Cell Biol 2005;37:33–7.

Gavard JA, Chaitman BR, Sakai S, Stocke K, Danchin N, Erhardt L, et al. Prognostic significance of elevated creatine kinase MB after coronary bypass surgery and after an acute coronary syndrome: results from the GUARDIAN trial. J Thorac Cardiovasc Surg 2003;126:807–13.

Haist JV, Hirst CN, Karmazyn M. Effective protection by NHE-1 inhibition in ischemic and reperfused heart under preconditioning blockade. Am J Physiol Heart Circ Physiol 2003;284:H798–803.

Kashihara K, Kawada T, Li M, Sugimachi M, Sunagawa K. Bezold–Jarisch reflex blunts arterial baroreflex via the shift of neural arc toward lower sympathetic nerve activity. Jpn J Physiol 2004;54:395–404.

Kitagawa H, Yamazaki T, Akiyama T, Sugimachi M, Sunagawa K, Mori H. Microdialysis separately monitors myocardial interstitial myoglobin during ischemia and reperfusion. Am J Physiol Heart Circ Physiol 2005;289:H924–30.

Klein HH, Pich S, Bohle RM, Lindert-Heimberg S, Nebendahl K. Na^+/H^+ exchange inhibitor cariporide attenuates cell injury predominantly during ischemia and not at onset of reperfusion in porcine hearts with low residual blood flow. Circulation 2000;102:1977–82.

Kristo G, Yoshimura Y, Ferraris SP, Jahania SA, Mentzer Jr RM, Lasley RD. The preischemic combination of the sodium–hydrogen exchanger inhibitor cariporide and the adenosine agonist AMP579 acts additively to reduce porcine myocardial infarct size. J Am Coll Surg 2004;199:586–94.

Kurz T, Richardt G, Hagl S, Seyfarth M, Schömig A. Two different mechanisms of noradrenaline release during normoxia and simulated ischemia in human cardiac tissue. J Mol Cell Cardiol 1995;27:1161–72.

Leineweber K, Heusch G, Schulz R. Regulation and role of the presynaptic and myocardial Na^+/H^+ exchanger NHE1: effects on the sympathetic nervous system in heart failure. Cardiovasc Drug Rev 2007;25:123–31.

Létienne R, Bel L, Bessac AM, Denais D, Degryse AD, John GW, et al. Cardioprotection of cariporide evaluated by plasma myoglobin and troponin I in myocardial infarction in pigs. Fundam Clin Pharmacol 2006;20:105–13.

Linz W, Albus U, Crause P, Jung W, Weichert A, Schölkens BA, et al. Dose-dependent reduction of myocardial infarct mass in rabbits by the NHE-1 inhibitor cariporide (HOE642). Clin Exp Hypertens 1998;20:733–49.

Miura T, Ogawa T, Suzuki K, Goto M, Shimamoto K. Infarct size limitation by a new $Na(+)$-H^+ exchange inhibitor, HOE642: difference from preconditioning in the role of protein kinase C. J Am Coll Cardiol 1997;29:693–701.

Nuñez IP, Fantinelli J, Arbeláez LF, Mosca SM. Mitochondrial KATP channels participate in the limitation of infarct size by cariporide. Naunyn Schmiedebergs Arch Pharmacol 2011;383:563–71.

Reffelmann T, Kloner RA. Is microvascular protection by cariporide and ischemic preconditioning causally linked to myocardial salvage? Am J Physiol Heart Circ Physiol 2003;284:H1134–41.

Schömig A, Haass M, Richardt G. Catecholamine release and arrhythmias in acute myocardial ischaemia. Eur Heart J 1991;12(Suppl. F):38–47.

Zeymer U, Suryapranata H, Monassier JP, Opolski G, Davies J, Rasmanis G, et al. The Na^+/H^+ exchange inhibitor eniporide as an adjunct to early reperfusion therapy for acute myocardial infarction. Results of the evaluation of the safety and cardioprotective effects of eniporide in acute myocardial infarction (ESCAMI) trial. J Am Coll Cardiol 2001;38:1644–50.

Molecular Genetics & Genomic Medicine

Open Access

ORIGINAL ARTICLE

Mutations of *NOTCH3* in childhood pulmonary arterial hypertension

Ayako Chida[1,2], Masaki Shintani[2], Yoshihisa Matsushita[2], Hiroki Sato[3], Takahiro Eitoku[4], Tomotaka Nakayama[5], Yoshiyuki Furutani[2], Emiko Hayama[2], Yoichi Kawamura[1], Kei Inai[2], Shinichi Ohtsuki[4], Tsutomu Saji[5], Shigeaki Nonoyama[1] & Toshio Nakanishi[2]

[1]Department of Pediatrics, National Defense Medical College, 3-2 Namiki, Tokorozawa, Saitama, 359-8513, Japan
[2]Department of Pediatric Cardiology, Tokyo Women's Medical University, 8-1 Kawada-cho, Shinjuku-ku, Tokyo, 162-8666, Japan
[3]Department of Preventive Medicine and Public Health, National Defense Medical College, 3-2 Namiki, Tokorozawa, Saitama, 359-8513, Japan
[4]Division of Pediatric Cardiology, Department of Pediatrics, Okayama University, 2-5-1 Shikata-cho, Okayama, 700-8558, Japan
[5]Department of Pediatrics, Toho University Medical Center, Omori Hospital, 6-11-1 Omori-nishi, Ota-ku, Tokyo, Japan

Keywords
ER stress, gene mutation, *NOTCH3*, pulmonary arterial hypertension

Correspondence
Toshio Nakanishi, Department of Pediatric Cardiology, Tokyo Women's Medical University, 8-1 Kawada-cho, Shinjuku-ku, Tokyo, 162-8666, Japan. Tel: +81-3-3353-8112; Fax: +81-3-3352-3088;
E-mail: pnakanis@hij.twmu.ac.jp

Funding Information
This work was supported by MEXT KAKENHI grant number 24591588.

Received: 13 August 2013; Revised: 2 November 2013; Accepted: 12 November 2013

Molecular Genetics & Genomic Medicine **2014; 2(3): 229–239**

doi: 10.1002/mgg3.58

Abstract

Mutations of *BMPR2* and other TGF-β superfamily genes have been reported in pulmonary arterial hypertension (PAH). However, 60–90% of idiopathic PAH cases have no mutations in these genes. Recently, the expression of NOTCH3 was shown to be increased in the pulmonary artery smooth muscle cells of PAH patients. We sought to investigate *NOTCH3* and its target genes in PAH patients and clarify the role of NOTCH3 signaling. We screened for mutations in *NOTCH3*, *HES1*, and *HES5* in 41 PAH patients who had no mutations in *BMPR2*, *ALK1*, *endoglin*, *SMAD1/4/8*, *BMPR1B*, or *Caveolin-1*. Two novel missense mutations (c.2519 G>A p.G840E, c.2698 A>C p.T900P) in *NOTCH3* were identified in two PAH patients. We performed functional analysis using stable cell lines expressing either wild-type or mutant NOTCH3. The protein-folding chaperone GRP78/BiP was colocalized with wild-type NOTCH3 in the endoplasmic reticulum, whereas the majority of GRP78/BiP was translocated into the nuclei of cells expressing mutant NOTCH3. Cell proliferation and viability were higher for cells expressing mutant NOTCH3 than for those expressing wild-type NOTCH3. We identified novel *NOTCH3* mutations in PAH patients and revealed that these mutations were involved in cell proliferation and viability. NOTCH3 mutants induced an impairment in NOTCH3-HES5 signaling. The results may contribute to the elucidation of PAH pathogenesis.

Introduction

Pulmonary arterial hypertension (PAH) is a progressive, severe, potentially fatal disease with an estimated incidence of approximately 1–2 patients per million per year (Gaine and Rubin 1998). Idiopathic PAH (IPAH) is a sporadic form of the disease in which there is neither a family history of PAH nor an identified risk factor (Simonneau et al. 2009). Heritable PAH (HPAH) is inherited in an autosomal dominant fashion with 10–20% penetrance, and affects females approximately twice as often as males (Machado et al. 2009).

Bone morphogenetic protein (BMP) receptor 2 (*BMPR2*), a member of the transforming growth factor (TGF)-β superfamily, was identified as a primary gene for HPAH in 2000 (Deng et al. 2000; Lane et al. 2000). Subsequent studies of the TGF-β superfamily revealed additional genes responsible for PAH: activin receptor-like kinase 1 (*ALK1*), *endoglin* (*ENG*), *SMAD1/4/8*, and bone morphogenetic protein receptor 1B (*BMPR1B*) (Trembath et al. 2001; Harrison et al. 2003, 2005; Shintani et al. 2009; Chida et al. 2012; Nasim et al. 2012). In addition, Austin et al. (2012) identified *Caveolin-1* (*CAV1*) mutations in PAH patients using whole exome sequencing. These genetic studies have considerably enhanced our understanding of the molecular basis of PAH. However, almost 30% of HPAH cases and 60–90% of IPAH cases have no mutations in *BMPR2*, *ALK1*, *ENG*, *SMAD 1/4/8*, *BMPR1B*, or *CAV1*.

In 2009, Li et al. reported that human pulmonary hypertension could be characterized by the overexpression of NOTCH3 (OMIM 600276) in small pulmonary artery smooth muscle cells (SMCs), and that the severity of the disease in humans and rodents is correlated with the amount of NOTCH3 protein in the lungs (Li et al. 2009). Therefore, we hypothesized that genes belonging to the NOTCH3 signaling pathways, in addition to the BMP signaling pathway, may be associated with the onset of IPAH/HPAH. Accordingly, we screened for mutations in *NOTCH3* and its target genes, *HES1* and *HES5*.

Materials and Methods

Subjects

From a previous screen of patients with IPAH/HPAH (Shintani et al. 2009; Chida et al. 2012), we identified 41 patients who did not have mutation in *BMPR2*, *ALK1*, *SMAD1*, *SMAD4*, *SMAD8*, *BMPR1B*, or *CAV1*. These patients formed the basis of this study (Fig. 1). The diagnosis of IPAH/HPAH was made through a clinical evaluation, echocardiography, and cardiac catheterization based on the following criteria: mean pulmonary artery pressure >25 mmHg at rest (Galiè et al. 2009). Patients with PAH associated with another disease, such as portal hypertension or congenital heart disease, were excluded from this study by trained cardiologists. This study was approved by the Institutional Review Committee of Tokyo Women's Medical University. Written informed consent was obtained from all patients or their guardians in accordance with the Declaration of Helsinki.

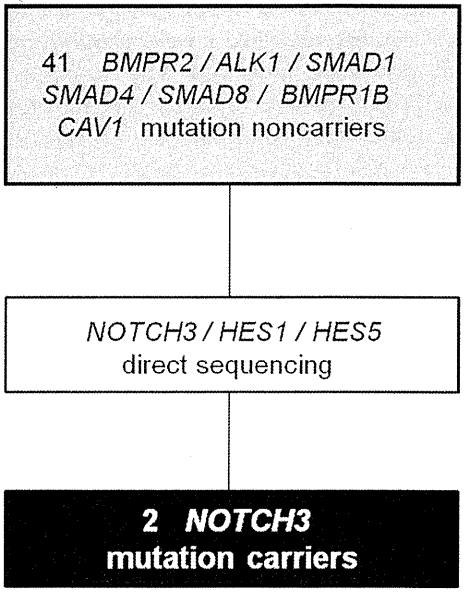

Figure 1. Patient disposition.

Molecular analysis

For the 41 patients with no mutations in *BMPR2*, *ALK1*, *SMAD 1/4/8*, *BMPR1B*, or *CAV1*, all coding exons and adjacent intronic regions for *NOTCH3*, *HES1*, and *HES5* were amplified from the genomic DNA using polymerase chain reactions (PCR primer details are available in Table S1). PCR-amplified products were purified and screened via bidirectional direct sequencing with an ABI 3130xl DNA Analyzer (Applied Biosystems, CA). All of the generated sequences were compared with wild-type *NOTCH3* (GenBank NM_000435), *HES1* (GenBank NM_005524), and *HES5* (GenBank NM_001010926).

Stable cell lines

We established stable HEK293 cell lines in which the expression of NOTCH3 was inducible using the tetracycline regulatory system because it was known that the expression of NOTCH3 in vascular SMCs caused excessive cell death as early as 2 days after transfection (Takahashi et al. 2010). T-REx 293 cells (Invitrogen, Carlsbad, CA) were grown in high glucose DMEM (Sigma, St Louis, MO) supplemented with 10% fetal bovine serum (Gibco, Grand Island, NY), 2 mmol/L L-glutamine, and 5 μg/mL blasticidin (Gibco). The wild-type and mutant NOTCH3 constructs were transfected into T-REx 293 cells using Lipofectamine 2000 reagent (Invitrogen). After 48 h, cells were selected in the presence of 100 μg/mL Zeocin and 5 μg/mL Blasticidin-S (Invitrogen). After treatment with tetracycline (Tet; 2 μg/mL) for 24 h, the expression level of NOTCH3 was determined by western blotting using AbN2. Stable cell lines were maintained in high glucose DMEM-containing 10% fetal bovine serum, 5 μg/mL Zeocin, and 5 μg/mL Blasticidin-S.

Preparation of plasmids, antibodies, and ligands

Human pcDNA4/TO-NOTCH3 was kindly provided by Dr. Atsushi Watanabe (Aichi, Japan). The reporter gene construct pHes5-luc was a kind gift from Dr. Ryoichiro Kageyama (Kyoto, Japan). Site-directed mutagenesis was carried out using a site-directed mutagenesis kit (Stratagene, CA). The antibodies used were as follows: rabbit polyclonal anti-human NOTCH3 antibodies (AbN2; gifts from A. Watanabe), monoclonal NOTCH3 antibody (3A2; gift from A. Watanabe), anti-β actin mouse antibody (Sigma-Aldrich, MO), anti-mouse ERp72 antibody, anti-mouse Calnexin antibody, and anti-mouse BiP/GRP78 antibody (R&D Systems, Oxon, UK). AbN2 and 3A2 have

previously been shown to specifically recognize the NOTCH3 protein (Takahashi et al. 2010). Recombinant human Jagged-1 Fc chimera and human BMP4 enzyme-linked immunosorbent assays were from R&D Systems.

Statistical analysis

Data are presented as means with standard deviation (SD). Differences between the means were evaluated by the Dunnett's test following one-way or two-way analysis of variance (ANOVA). Values of $P < 0.05$ were considered significant. All statistical analyses were performed using SAS version 9.3 (SAS Institute, Cary, NC).

The methods of western blotting and immunoprecipitation, immunocytochemistry, luciferase assay, and cell proliferation and viability tests are detailed in the Data S1.

Results

Identification of two novel *NOTCH3* mutations

We screened for mutations in the *NOTCH3*, *HES1*, and *HES5* genes in 41 IPAH/HPAH patients who had no mutations in *BMPR2*, *ALK1*, *ENG*, *SMAD1/4/8*, *BMPR1B*, or *CAV1* (Fig. 1). In these 41 patients, the median age at diagnosis was 9 years (range: 0–62 years). The number of male patients was 18 (44 %). Although no mutations were identified in *HES1* or *HES5*, we identified two *NOTCH3* missense mutations in two independent probands with IPAH: a c.2519 G>A p.G840E mutation in proband A, and a c.2698 A>C p.T900P mutation in proband B (Fig. 2A). As depicted in Figure 2B, NOTCH3 consists of 34 epidermal growth factor (EGF)-like repeats, three Notch/Lin-12 repeats, a transmembrane domain, seven ankyrin repeats, and a PEST sequence (rich in proline [P], glutamic acid [E], serine [S], and threonine [T]). Both the G840E and T900P mutations were located in the EGF-like repeats. The alignment of the NOTCH3 protein of nine distantly related species showed that the G840 and T900 amino acids were highly conserved (Fig. 2C). The G840E and T900P mutations were absent in 170 Japanese healthy controls and additional 300 Caucasian healthy controls and were not found in the 1000 Genomes Database (http://www.1000genomes.org) or the Exome Variant Server (EVS) Database (evs.gs.washington.edu/EVS). Besides, in Polyphen-2 (Polymorphism phenotyping v2) (Adzhubei et al. 2010) and the SIFT

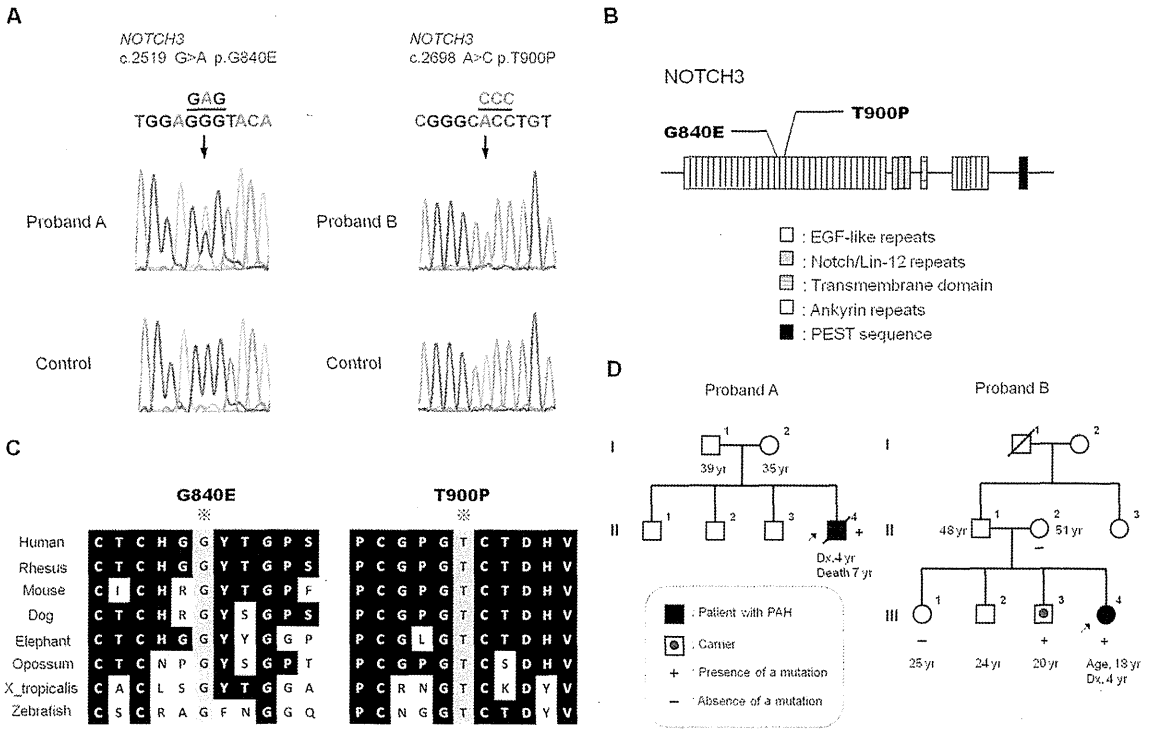

Figure 2. *NOTCH3* mutations in idiopathic pulmonary arterial hypertension patients. (A) Two mutations, c.2519 G>A p.G840E and c.2698 A>C p.T900P, were identified in two probands. (B) Schematic representation of the wild-type NOTCH3 protein and the locations of the two mutations. (C) Alignment of NOTCH3 proteins among human, rhesus monkey, mouse, dog, elephant, opossum, chicken, *Xenupus tropicalis*, and zebrafish, showing the conservation of glycine 840 and threonine 900 in these species. (D) Pedigrees of the patients' families. The current age or the age at diagnosis, as well as the age at diagnosis (Dx) is provided for each family member.

Human Protein (Kumar et al. 2009), both variants were regarded as "Probably damaging" and "Damaging," respectively.

In proband A, there was no family history of PAH (Fig. 2D). The subject's family members were not screened for *NOTCH3* mutations because their blood samples could not be obtained. Although there was no family history of PAH in proband B, the same mutation was identified in the patient's youngest elder brother (Figs. 2D and S1). The patient's mother and elder sister did not have the mutation. The other family members of proband B were not screened for *NOTCH3* mutations because their blood samples could not be obtained.

Clinical characteristics of patients

Proband A

When the patient was 4 years old, he visited the clinic because of upper respiratory inflammation. A physical examination revealed a cardiac murmur. Cardiomegaly was identified by a chest X-ray and the patient was diagnosed with IPAH. The hemodynamic data of the patient at 5 years of age revealed a mean pulmonary arterial pressure (mPAP) of 70 mmHg and a right atrial pressure (RAP) of 7 mmHg. The patient's condition progressed to the World Health Organization (WHO) functional class II at 5 years of age. The patient had been administered sildenafil, bosentan, beraprost, and warfarin since the age of 4. When he was 5 years old, the patient began home oxygen therapy (HOT) and diuretics. He did not receive epoprostenol because his family's consent was not obtained. The patient's condition deteriorated despite increases in the doses of sildenafil, bosentan, and veraprost. The patient suffered cardiopulmonary arrest caused by pulmonary hypertension crisis at 6 years old; he was successfully resuscitated and began intravenous epoprostenol therapy. Although the dose of epoprostenol was increased gradually, the patient's heart failure worsened. When he was 7 years old, the patient was discharged from hospital after beginning home intravenous epoprostenol. However, the patient died 9 days later because of a pulmonary hemorrhage.

The patient's past history included brain infarction and right hemiparesis caused by Moyamoya disease. The patient had left cerebral arterial revascularization surgery when he was 3 years old. No complications were reported in the aorta or renal arteries.

Proband B

This patient's first symptom was fatigue at 4 years of age. At the initial visit, the patient's right ventricle pressure was almost equal to left ventricle pressure and her brain natriuretic peptide level was 1380 pg/mL. Although the patient was administered beraprost, she became more impaired, and began intravenous epoprostenol at the age of 5. This therapy was initially very effective; however, the patient's mPAP progressively increased. Increasing the amount of epoprostenol and administering sildenafil and bosentan were not effective. The patient's hemodynamic data at 15 years of age revealed an mPAP of 67 mmHg, a RAP of 12 mmHg, a CI of 2.9 L min^{-1} m^{-2}, and a pulmonary artery wedge pressure of 12 mmHg. The patient has been receiving intravenous epoprostenol, home oxygen therapy, sildenafil, bosentan, cardiotonic drugs, anticoagulants, and diuretics. The current condition of the patient at 18 years old is WHO functional class III. Currently, the patient and her family do not wish to undergo lung transplantation.

The patient's history includes Graves' disease, which occurred at 13 years old. She initially received thiamazole; however, she stopped that treatment and began potassium iodide because of agranulocytosis. Thyroidectomy was not approved because of severe PH.

Decreased expression of NOTCH3 and ER-Resident chaperones in mutant cell lines

According to a previous report (Takahashi et al. 2010), we established stable HEK293 cell lines in which the expression of NOTCH3 was inducible using the tetracycline-on (Tet-on) regulatory system (T-REx System; Invitrogen). Several cell lines were established, and three cell lines for each construct were selected for NOTCH3 expression experiments. The expression of the mutant versions of NOTCH3 was lower than that of wild-type NOTCH3 (Fig. 3). Additionally, the expression levels of three endoplasmic reticulum (ER)-resident chaperones, GRP78/BiP, Calnexin, and ERp72, were higher in cells overexpressing wild-type NOTCH3 than in cells overexpressing the NOTCH3 mutants, particularly for the T900P-NOTCH3 mutant (Figs. 3A and S2). In Figure S3, the mutant NOTCH3 protein disappeared more quickly than wild-type NOTCH3 protein. Based on the result, the lower expression levels of mutant NOTCH3 in Figure 3A were caused by the high clearance speed.

NOTCH3 mutants fail to fully bind to GRP78/BiP

On the basis of the findings illustrated in Figure 3A, we investigated whether mutant NOTCH3 interacts with ER chaperones. As shown in Figure 3B, GRP78/BiP coimmunoprecipitated with wild-type NOTCH3, indicating

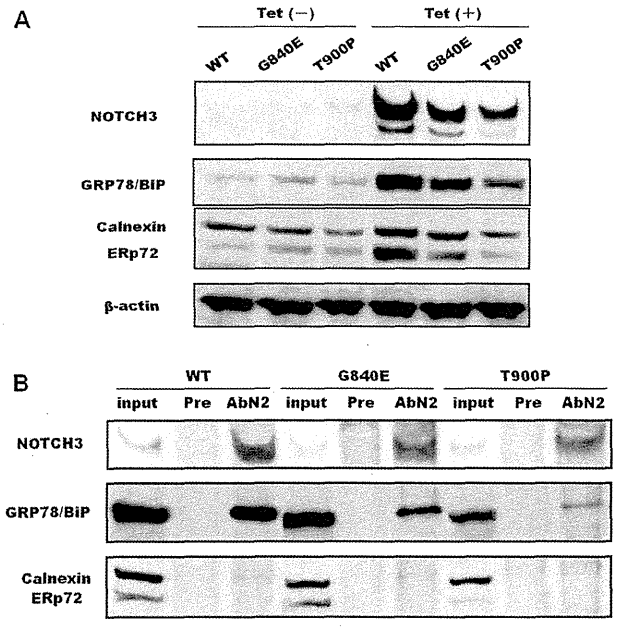

Figure 3. Expression of NOTCH3 and the endoplasmic reticulum (ER) chaperones. (A) Stable cells were incubated with or without 2 μg/mL tetracycline (Tet) for 24 h and these cell lysates (12 μg) were subjected to SDS-gel electrophoresis. We assessed more than three stable cell lines for each of the wild-type and mutant NOTCH3 proteins. The experiment was performed three times. (B) Interaction between ER chaperones and NOTCH3. Cell lysates (200 μg) from stable cell lines were subjected to immunoprecipitation using an anti-NOTCH3 antibody (AbN2) or preimmune rabbit IgG (Pre). Immunoprecipitated complexes were subjected to SDS-PAGE and western blotting. The experiments were performed in triplicate for each stable cell line (WT-17, G840E-36, and T900P-33).

that wild-type NOTCH3 interacted with this ER chaperone. The amount of GRP78/BiP that coprecipitated with the NOTCH3 mutants was markedly lower than the amount that coprecipitated with wild-type NOTCH3. Calnexin and ERp72 were not detected in any of the wild-type or mutant NOTCH3-immunoprecipitated samples.

Changes in NOTCH3 levels and GRP78/BiP localization

We examined the quantity and localization of wild-type or mutant NOTCH3 via immunostaining using the ER marker GRP78/BiP. While many wild-type NOTCH3 aggregates were detected in the perinuclear region of the cytoplasm, very few mutant NOTCH3 perinuclear aggregates were detected, particularly in cells transfected with T900P-NOTCH3 (Fig. 4A). Aggregates were colocalized with GRP78/BiP in cells expressing wild-type NOTCH3. However, in cells expressing G840E-NOTCH3, GRP78/BiP was partly localized in the nucleus and did not fully colocalize with NOTCH3 aggregates. This was particularly evident in cells expressing T900P-NOTCH3. When present in the nucleus, GRP78/BiP was colocalized with nuclear bodies (Fig. 4A).

Clearance of NOTCH3 aggregates

We next examined the degradation of wild-type and mutant NOTCH3 aggregates after 2 days using Tet-on cells. Figure 4B shows that wild-type NOTCH3 and G840E-NOTCH3 aggregates degraded slowly, whereas T900P-NOTCH3 aggregates disappeared rapidly. As was the case for stable cells immediately after Tet-on, GRP78/BiP was located in the nucleus in cells expressing mutant NOTCH3, most notably in cells expressing T900P-NOTCH3. These findings were confirmed by western blotting of cells expressing NOTCH3 (Fig. S3).

Promotion of cell proliferation and viability by mutant NOTCH3 expression

Cell proliferation was assessed by cell counting at 1 day, 3 days, and 5 days after Tet-on. The expression of wild-type NOTCH3 in the Tet-on cells caused a decrease in cell number compared to the untreated cells; however, the expression of mutant NOTCH3 had little impact on cell growth (Fig. 5A). We evaluated the ratio of the number of Tet-on cells to that of untreated cells on day 5 (Fig. 5A). The ratio of G840E-36 (0.78 ± 0.05) and T900P (0.70 ± 0.10) were significantly higher than that of WT-17 (0.50 ± 0.04, $P = 0.004$ and 0.021, respectively). These findings were confirmed via a cell proliferation assay using the WST-1 reagent (Fig. 5B and 5C). While the cells expressing wild-type NOTCH3 showed viability that was equivalent to that of untreated cells, the cells expressing mutant NOTCH3 exhibited a significantly higher level of viability. These cells reached confluence and did not show any detectable apoptosis or morphological abnormalities.

The NOTCH3 mutant induces the downregulation of NOTCH3-HES5 signaling activity

We investigated the transcriptional activity mediated by wild-type or mutant NOTCH3 with or without Jagged-1 to determine whether mutant NOTCH3 could increase or decrease NOTCH3-responsive target gene activity. To this end, we used a pHes5-luc reporter, where the luciferase Hes5 promoter drives expression to assess NOTCH3 activity. The luciferase assay showed that wild-type NOTCH3 exhibited significantly higher luciferase activity

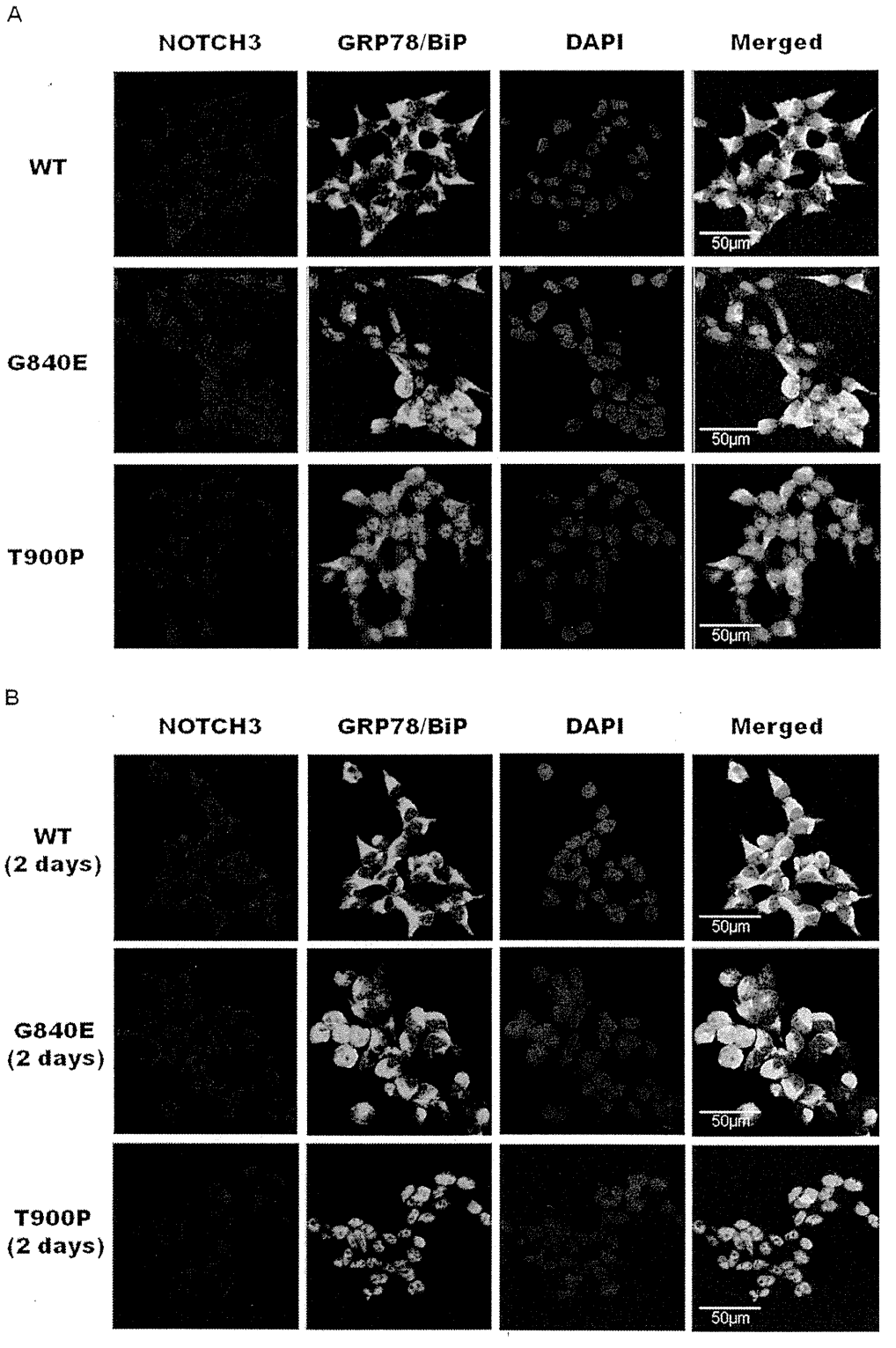

Figure 4. Changes in the quantity of NOTCH3 aggregates and the localization of GRP78/BiP. (A) Nine stable cell lines (WT-17, WT-21, WT-38, G840E-5, G840E-21, G840E-36, T900P-14, T900P-28, and T900P-33) were treated with 2 μg/mL tetracycline for 24 h and double-stained with an anti-Notch3 antibody (AbN2) and a GRP78/BiP antibody. NOTCH3 (red) was detected by an Alexa Fluor 568-labeled secondary antibody and GRP78/BiP (green) was detected by an Alexa Fluor 488-labeled secondary antibody. (B) Stable cells were treated with tetracycline for 24 h and then incubated without tetracycline for 2 days. Cells were double-stained as described above.

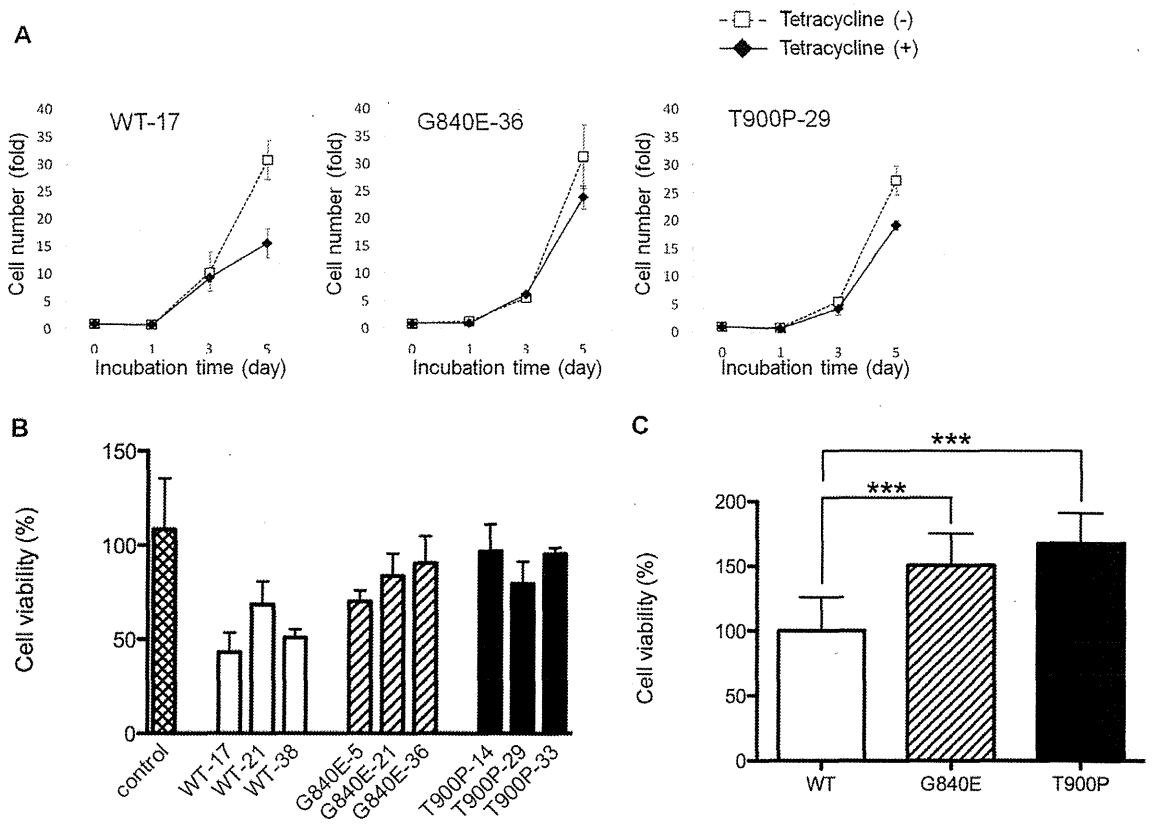

Figure 5. Cell proliferation and viability of NOTCH3. (A) Stable cells were incubated with (closed argyles) or without (open squares) tetracycline and harvested on days 0, 1, 3, and 5 for each of the nine stable cell lines (WT-17, WT-21, WT-38, G840E-5, G840E-21, G840E-36, T900P-14, T900P-29, and T900P-33). Each data point represents the mean number of cells with the standard deviation from four independent experiments. (B) Stable cells were incubated with or without tetracycline for 3 days. Cell viability was determined using the WST-1 reagent. The control indicates T-REx 293 cells that were not transfected. Values represent the means with the standard deviation from three independent experiments and are shown as the percentage of the total number of cells without tetracycline treatment. (C) The cell viability demonstrated in (B) was converted to a percentage of the mean value relative to that of stable cells expressing wild-type NOTCH3. Each data point represents the mean and standard deviation from nine cell lines. ***$P < 0.001$.

with Jagged-1 stimulation than without Jagged-1 stimulation. After stimulation with Jagged-1, however, G840E-NOTCH3 and T900P-NOTCH3 did not induce higher activity than mutant NOTCH3 without Jagged-1 stimulation (Fig. 6). These findings indicated that NOTCH3 mutants induced an impairment in NOTCH3-HES5 signaling.

Discussion

This is the first study to report the identification of two missense mutations in *NOTCH3* in IPAH patients. Both of the mutations identified in this study result in amino acid substitutions in the highly conserved and functionally essential EGF-like domain, and both mutations were absent in 170 Japanese and 300 Caucasian healthy controls, the 1000 Genomes Database, and the EVS Database.

NOTCH genes encode a group of 300-kD single-pass transmembrane receptors (*NOTCH1–4*). The large extracellular domain contains tandem EGF-like repeats and cysteine-rich Notch/LIN-12 repeats, and Ankyrin repeats and a PEST sequence have been found within the intracellular domain (ICD) (Artavanis-Tsakonas et al. 1999). The NOTCH signaling pathway is highly evolutionarily conserved and is critical for cell fate determination during embryonic development, including many aspects of vascular development (Wang et al. 2008). Upon interacting with its ligands (Jagged-1, Jagged-2, and Delta family) expressed on neighboring cells, NOTCH undergoes proteolytic cleavage, which frees the ICD from the plasma membrane (Xia et al. 2012). This change induces translocation of the ICD into the nucleus. The ICD then forms a complex with the transcriptional repressor CBF1/RBP-jk, which induces the transcription of downstream target genes, including

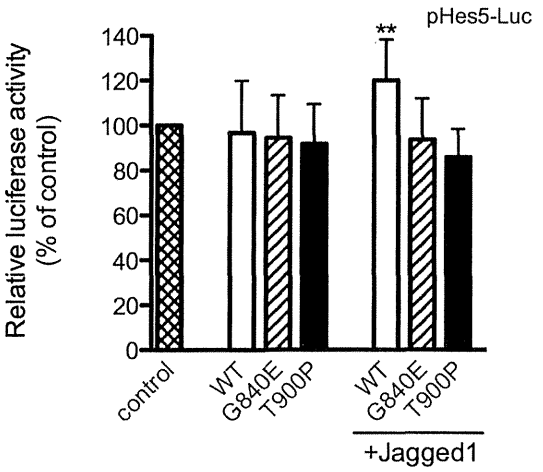

Figure 6. Luciferase activity induced by *NOTCH3*. T-REx 293 cells were transfected with pHes5-Luc and any one of wild-type NOTCH3, mutant NOTCH3, or the empty pcDNA4/TO vector. Some of the cells were cultured with preclustered Jagged-1 Fc (100 ng/mL) for 4 h. Values represent the mean with standard deviation of four independent experiments. The means were compared with wild-type (WT without stimulation with Jagged-1) using one-way ANOVA followed by Dunnett's test. $^{**}P < 0.01$.

HES1/5/7 and the *HEY* family genes (Iso et al. 2003; Weber 2008).

NOTCH3 is predominantly expressed in arterial vascular SMCs, where it regulates SMC differentiation (Zhu et al. 2011; Xia et al. 2012). The main NOTCH3 ligand is Jagged-1, which is also expressed in arterial endothelial cells (ECs) (Xia et al. 2012). Taking these reports into consideration, we decided to perform functional analysis of mutant NOTCH3 through the use of Jagged-1 Fc.

NOTCH3 mutations are known to be associated with cerebral autosomal dominant arteriopathy with subcortical infarcts and leukoencephalopathy (CADASIL) (Joutel et al. 1996). More than 150 *NOTCH3* mutations have been reported in CADASIL patients; mutation hot spots are located in exons 3 and 4 (Chabriat et al. 2009). Both of the *NOTCH3* mutations that we identified in IPAH patients were missense mutations located in exons 16 and 17. To date, no mutations in these two exons have been reported in CADASIL patients, and there have been no reports of a PAH complication in CADASIL.

In this study, we revealed that compared to the wild-type protein, mutant NOTCH3 formed aggregates poorly and decreased the amount of GRP78/BiP, Calnexin, and ERP72. Our immunoprecipitation studies suggested that GRP78/BiP cannot interact with mutant NOTCH3. In addition, we found that T900P-NOTCH3 was degraded more rapidly than wild-type NOTCH3. These findings are not consistent with a previous report that investigated CADASIL mutations using similar methods (Takahashi et al. 2010); however, these differences may be attributable to the difference in the location of the mutations.

In an immunocytochemistry study, we indicated that GRP78/BiP and wild-type NOTCH3 were colocalized in the ER, and that GRP78/BiP was localized in the nuclei of cells expressing mutant NOTCH3. GRP78, a member of the HSP70 gene family, has been traditionally regarded as a major ER chaperone that facilitates protein folding and assembly, protein quality control, Ca^{2+} binding, and the regulation of ER stress signaling (Ni et al. 2011). It is also known that GRP78 can be observed in the nucleus when it is ectopically overexpressed or induced by ER stress (Reddy et al. 2003; Huang et al. 2009). On the basis of this information, we hypothesize that the mutant NOTCH3 protein induces a high level of stress on the ER and induces GRP78/BiP nuclear translocation. Because the mutant NOTCH3 protein is located in the ER, it may not be able to interact with GRP78/BiP in the nucleus. Gene mutations can cause aberrant protein folding and the accumulation of the mutant protein in the ER (Takahashi et al. 2010). Because ER chaperones facilitate ER-associated protein degradation to clear aggregated, misfolded, or unassembled proteins (Ni and Lee 2007), T900P-NOTCH3 proteins may be degraded more rapidly than wild-type NOTCH3.

The cells expressing mutant NOTCH3 showed higher levels of viability and proliferation than the cells expressing wild-type NOTCH3, and did not exhibit apoptosis or morphological abnormalities. These findings suggest that when the normal NOTCH3 protein is absent, increases in cell proliferation rates occur. This result is contrary to the work of Li et al. and taken together the role of NOTCH3 may be more complex than first described. Thus more work is required to resolve this discrepancy.

In the luciferase assay, we showed that the *NOTCH3* mutations we identified caused an impairment in NOTCH3-HES5 signaling activity. It remains unclear whether the *NOTCH3* mutations identified in this study affect NOTCH signaling activity. One study revealed that a part of the mutations identified in CADASIL patients caused a gain in function in the NOTCH signaling pathway (Joutel et al. 2004). Another report indicated that *NOTCH3* mutations in or near the ligand-binding site (EGF-like repeats 10-11, corresponding to a part of exon 7-9) impaired ligand binding sufficiently to affect signaling activity (Peters et al. 2004). Furthermore, another two studies suggested that most of the mutations located outside of the ligand-binding site did not impair the signal transduction activity of NOTCH3 (Low et al. 2006; Monet-Leprêtre et al. 2009). The difference in function

between exon 16–17, in which the mutations we identified were located, and other exons corresponding to EGF-like repeats remain unexplained. Further investigations are necessary.

It appears that epoprostenol may not be sufficiently effective in the two PAH patients with *NOTCH3* mutations. Although the reason remains unclear, epoprostenol might not influence to NOTCH signaling. In addition, their age at diagnosis was very young comparatively. It was difficult to identify other additional phenotypic features in the two subjects. The youngest elder brother of proband B has the same *NOTCH3* mutation, but has not exhibited any clinical signs of PAH to date. The *NOTCH3* mutation may have very low penetrance in familial PAH, as well as *BMPR2* mutation in familial PAH. In CADASIL patients, the penetrance of *NOTCH3* mutation is complete by the end of fourth decade (Ayata 2010). Although we cannot clarify whether the youngest elder brother of proband B will develop PAH in the future, it will be necessary to check his health condition periodically.

We identified several limitations of our study. For the *NOTCH3* mutations we identified, a detailed investigation in a larger number of subjects is needed, and a search for mutations of other NOTCH3 pathway genes may also be beneficial. Moreover, although we demonstrated that the mutant NOTCH3 reduced the amount of GRP78/BiP, Dromparis et al. (2013) reported that the expression of GRP78 was increased in chronic normobaric hypoxia-pulmonary hypertension mice. These differences may be a result of the different types of mutations, cells, or species used in the various studies. We acknowledge that the HEK293 cells we used are not the ideal cell lines for functional studies of PAH; thus, it is difficult to prove definitively that NOTCH3 causes PAH based on our findings. However, in the study conducted by Dromparis et al. (2013), it seems that GRP78 was translocated to the nucleus in the pulmonary artery SMCs of hypoxia mice more than normoxia mice. Because this finding is consistent with our immunostaining results, the study supports our hypothesis that mutant NOTCH3 induces a high degree of ER stress. Therefore, additional investigations are necessary to further analyze the function of *NOTCH3* in the pathogenesis of PAH. These studies might include cell proliferation and viability analyses using both ECs and SMCs from human pulmonary arteries and animal models with the *NOTCH3* mutation.

Acknowledgments

We are grateful to the patients and their family members. We thank Atsushi Watanabe and Ryoichiro Kageyama for providing the plasmids. We thank Ryohei Tsutsumi for his excellent technical assistance. We also thank Rumiko Matsuoka for her supervision.

Conflict of Interest

None declared.

References

Adzhubei, I. A., S. Schmidt, L. Peshkin, V. E. Ramensky, A. Gerasimova, P. Bork, et al. 2010. A method and server for predicting damaging missense mutations. Nat. Methods 7:248–249.

Artavanis-Tsakonas, S., M. D. Rand, and R. J. Lake. 1999. Notch signaling: cell fate control and signal integration in development. Science 284:770–776.

Austin, E. D., L. Ma, C. LeDuc, E. Berman Rosenzweig, A. Borczuk, J. A. Phillips, III, et al. 2012. Whole exome sequencing to identify a novel gene (caveolin-1) associated with human pulmonary arterial hypertension. Circ. Cardiovasc. Genet. 5:336–343.

Ayata, C. 2010. CADASIL: experimental insights from animal models. Stroke 41(10 Suppl.):S129–S134.

Chabriat, H., A. Joutel, M. Dichgans, E. Tournier-Lasserve, and M. G. Bousser. 2009. Cadasil. Lancet Neurol. 8:643–653.

Chida, A., M. Shintani, T. Nakayama, Y. Furutani, E. Hayama, K. Inai, et al. 2012. Missense mutations of the *BMPR1B* (*ALK6*) gene in childhood idiopathic pulmonary arterial hypertension. Circ. J. 76:1501–1508.

Deng, Z., J. H. Morse, S. L. Slager, N. Cuervo, K. J. Moore, G. Venetos, et al. 2000. Familial primary pulmonary hypertension (gene *PPH1*) is caused by mutations in the bone morphogenetic protein receptor-II gene. Am. J. Hum. Genet. 67:737–744.

Dromparis, P., R. Paulin, T. H. Stenson, A. Haromy, G. Sutendra, and E. D. Michelakis. 2013. Attenuating endoplasmic reticulum stress as a novel therapeutic strategy in pulmonary hypertension. Circulation 27:115–125.

Gaine, S. P., and L. J. Rubin. 1998. Primary pulmonary hypertension. Lancet 352:719–725.

Galiè, N., M. M. Hoeper, M. Humbert, A. Torbicki, J. L. Vachiery, J. A. Barbera, et al. 2009. Guidelines for the diagnosis and treatment of pulmonary hypertension: the Task Force for the Diagnosis and Treatment of Pulmonary Hypertension of the European Society of Cardiology (ESC) and the European Respiratory Society (ERS), endorsed by the International Society of Heart and Lung Transplantation (ISHLT). ESC Committee for Practice Guidelines (CPG). Eur. Heart J. 30:2493–2537.

Harrison, R. E., J. A. Flanagan, M. Sankelo, S. A. Abdalla, J. Rowell, R. D. Machado, et al. 2003. Molecular and functional analysis identifies ALK-1 as the predominant cause of pulmonary hypertension related to hereditary haemorrhagic telangiectasia. J. Med. Genet. 40:865–871.

